DEVELOPMENT AND CHARACTERIZATION OF SHAPE MEMORY THERMOPLASTIC POLYURETHANE (TPU)/POLYLACTIC ACID (PLA) POLYMER BLEND

YUELEI GUO

A DISSERTATION SUBMITTED TO

THE FACULTY OF GRADUATE STUDIES

IN PARTIAL FULFILLMENT OF THE REQUIREMENTS

FOR THE DEGREE OF

DOCTOR OF PHILOSOPHY

GRADUATE PROGRAM IN MECHANICAL ENGINEERING

YORK UNIVERSITY

TORONTO, ONTARIO

Feb 2024

ABSTRACT

Shape memory polymers (SMPs) are a type of smart material that are gaining increasing attention nowadays. SMPs are enabled to realize dual shape transitions by applying a desired stimulus. The first shape is the permanent shape obtained during sample preparation, while the second shape represents the programmed shape imposed by the external force. And the most commonly used triggering stimuli include heat, electric, light, etc.

Among the various SMPs, the thermoplastic polyurethane (TPU)/polylactic acid (PLA) polymer blend is one of the favored picks for research. Some of the drawbacks of PLA, such as brittleness and low elongation, can be effectively improved by blending with TPUs. And the resulting TPU/PLA SMP present both enhanced mechanical properties and biocompatibility. Consequently, it shows a continuously growing market potential, especially in the biomedical field.

This study provides a thorough understanding of the working mechanism of the TPU/PLA polymer blend and the interacting effects upon some key microstructures. A total of four parts are covered in this study. The first part focuses on a fundamental study of the ratio of the two components. The role of the regions present in the polymer blend is analyzed and their respective functions in the realization of the shape memory effect are described. The second part of the study would be devoted to the examination of a factor that is easily overlooked by researchers, the

stretching time in the SM test. This leads to a number of microstructural changes, especially in the crystallization behaviors. And all corresponding alterations in shape memory properties could be observed and characterized. When comes to the third part, another parameter, the cooling method used in the fabrication process, is chosen to be investigated. As this factor also primarily contributes to the crystallization, a distinction is made between the role of crystals in this case and in the second part. Lastly, h-BN, a relatively innovative filler in the field of shape memory, has been added to prepare the TPU/PLA/BN polymer composite. The addition of h-BN extends the interpretation of the shape memory effect in the polymer composite with fillers.

ACKNOWLEDGEMENTS

I would like to express my sincere gratitude to my supervisor, Prof. Siu Ning Leung, for his invaluable guidance and endless support throughout my studies. It was a precious experience for working in his group.

I am also grateful to my committee members, Prof. George Zhu and Prof. Garrett Melenka, for their insightful and constructive feedback at the annual committee meetings. My special thanks also go to Prof. John Lam and Prof. Irina Garces for their kind suggestions as my examiners.

Thank you to my beloved family and friends who have provided support, understanding and encouragement through the highs and lows of these years. Thanks to my mom and dad for your endless love. Your confidence in me always inspired me and was my strongest backbone.

Finally, thanks to my persistence and efforts in this journey. A temporary end also signifies a new beginning. The future is unknown, so keep on going. All the best.

TABLE OF CONTENTS

LIST OF TABLES

LIST OF FIGURES

LIST OF ABBREVIATIONS

CNT	Carbon Nanotube
h-BN	Hexagonal Boron Nitride
MWCNT	Multiwalled carbon nanotube
PEG	Polyethylene Glycol
PLA	Polylactic Acid
SMM	Shape Memory Material
SMA	Shape Memory Alloy
SMP	Shape Memory Polymer
TPU	Thermoplastic Polyurethane

Chapter 1. Introduction

1.1 Preamble

Shape memory materials (SMMs), which represent a class of smart material, have been extensively researched in both academia and industry for decades. As a representative type of SMMs, shape memory polymers (SMPs) have been receiving more and more attention due to their excellent characteristics such as low cost, high degree of deformation, light weight, and good processability. SMPs represent a class of materials that are capable of dual-shape conversion between the original shape and the temporary or programmed shape under specific stimuli. Nowadays, a variety of SMPs have been widely used in broad areas, including but not limited to sensors, aerospace, biomedical devices, and textiles.

Thermoplastic polyurethane (TPU) is widely utilized in the development and investigation of SMPs due to its elasticity, flexibility, and biocompatibility. However, its low mechanical strength restricts its growth. Polylactic acid (PLA), on the other hand, features high strength as well as good biocompatibility and biodegradability. Therefore, polymer blends combining TPU and PLA have been developed, which present an improved overall mechanical performance and have great potential in a number of areas, especially in the biomedical field. While literatures have

reported studies on the design and fabrication of SMP based on TPU/PLA blend, the underlying mechanism of various governing factors have yet been elucidated. Therefore, this dissertation aims to focus on conducting systematical investigations to fill the knowledge and technological gaps of this promising SMP material system.

1.2 Scientific and Technological Gaps

Extensive research has been conducted on TPU/PLA polymer blends to investigate the effects of different material and processing parameters on their shape memory performances. These parameters include material compositions, programming temperature, and recovery temperature. Other researchers also investigated different processing strategies such as supercritical carbon dioxide foaming or additive manufacturing to prepare TPU/PLA-based SMPs and their resultant shape memory behaviours. Moreover, the addition of electrically conductive fillers (e.g., graphene oxide, carbon nanotubes, carbon black) were studied in attempt to convert the thermally-actuated SMP into electrically-actuated SMP. The incorporation of a third polymer component (e.g., polyethylene glycol) was also investigated to tune the activation temperature of the SMP to satisfy the requirement in some biomedical applications.

However, there was still limited discussion on the effects of the aforementioned parameters on the microstructure of TPU/PLA-based SMP and how such changes in microstructure affects the

shape memory properties. In particular, it is well known that both material and processing parameters would influence the crystallization behaviours of PLA. The crystallization behaviours of PLA are hypothesized to play a critical role in the shape memory behaviour and the working mechanism of the TPU/PLA SMP system. In addition, the correlations of different governing parameters on PLA's crystallization behaviours and thereby the blend system's shape memory properties were scarcely studied. Attempts should also be made to study other parameters that may affect the crystallization behaviours of PLA in the blend. Therefore, comprehensive research is needed to fill these knowledge and technological gaps in order to realize the full potential of using TPU/PLA blends as SMPs in various applications.

1.3 Research Objectives

The overarching goal of this study is to investigate the effects of different material and processing parameters on the shape memory properties of TPU/PLA blend. In addition, it aims to provide new insights to explain the mechanism of the TPU/PLA-based SMPs through the elucidation of the processing-structure-properties relationship of the blend system. In this context, there are four main objectives in this research:

1) Investigate the effects of different material and processing parameters on the shape memory performance (i.e., fixity and recovery) of the fabricated TPU/PLA-based SMP.

These include the TPU-to-PLA ratio, the stretching time during the shape memory testing cycle, the cooling rates during the fabrication, and the addition of a thermally conductive filler (i.e. hexagonal boron nitride);

2) Elucidate the influence of the aforementioned parameters on the microstructure of TPU/PLA blends. In particular, an emphasis will be made to investigate how these parameters change the crystallization behaviours of PLA in the blend.

3) Explore the correlation of different material and processing parameters on their influence of the structure and shape memory properties.

4) Identify the roles of different components (i.e., TPU, PLA, and hBN) as well as their different phases (e.g., amorphous and crystalline phases of PLA) on the shape memory behaviours of the SMP system and derive the mechanism that explains the behaviours of this class of SMP.

1.4 Overview of the Thesis

This dissertation is organized into eight chapters. A brief description of each chapter is given below.

Chapter 1 presents an overview of the scope of this dissertation, including a concise introduction to the subject of TPU/PLA-based SMPs, the technology gaps that remain to be filled,

and the research objectives of this study.

Chapter 2 reports a comprehensive literature survey on relevant research topics related to this dissertation. It starts with the discussion about the development of shape memory materials, including the progress of shape memory alloys and SMPs. This is followed by the classification of SMPs and the working principle of their shape memory effects. Lastly, it shifts the focus to previous research on the design and fabrication of TPU/PLA polymer blends as SMPs.

Chapter 3 outlines the experimental methodology of this study. This includes material selection, design of experiments, fabrication process of TPU/PLA blends and their composites, as well as characterization methods with detailed testing procedures.

Chapters 4 through 7 report the effects of different parameters on the microstructure and thereby the shape memory properties of TPU/PLA blends. A complete set of characterization has been performed for each of these parameters.

Chapter 4 investigates TPU/PLA polymer blends prepared with different compositions. The roles of TPU and PLA on the residue stress after the programming steps to store the temporary shape of the SMP and the resultant shape memory performance are discussed.

Chapter 5 presents the holding time during stretching at the deformation temperature as the factor for demonstrated in this chapter. In the testing of shape memory effect, polymer blends are stretched at different holding times and these polymer blends are characterized respectively.

In Chapter 6, TPU/PLA polymer blends fabricated by different cooling rates are discussed. The procedures to impose the different cooling rates are described in the chapter. The effects of cooling rate on the crystallization of PLA and thereby on the shape memory behaviours are presented.

Chapter 7 extends the study to TPU/PLA blend composite by adding hexagonal boron nitride (h-BN) as a thermally conductive filler. Polymer composites consist of equal weight of TPU and PLA with different h-BN contents of h-BN as well as those consist of 10 wt% of h-BN and different TPU-to-PLA ratios have been studied.

Chapter 8 is the summary chapter of the dissertation. In this chapter, the main contributions of this study are described. In addition, an outlook is provided to give recommendations to other researchers on potential directions to further advance this research area.

Chapter 2. Literature Review

2.1 Shape Memory Materials

Shape memory materials (SMMs) fulfill the ability to 'remember' their own permanent shapes from the temporary programmed shapes in response to designated stimulation. [1,2] As shown in Figure 2.1, the material holds an original shape initially. Subsequently, it is programmed to a desired temporary shape, and then can transform back to its original shape when activated by certain external stimuli. This behavior is generalized to the shape memory effect, which is an important factor in the assessment of SMM. Typical types of SMM include shape memory alloy (SMA) and shape memory polymer (SMP).

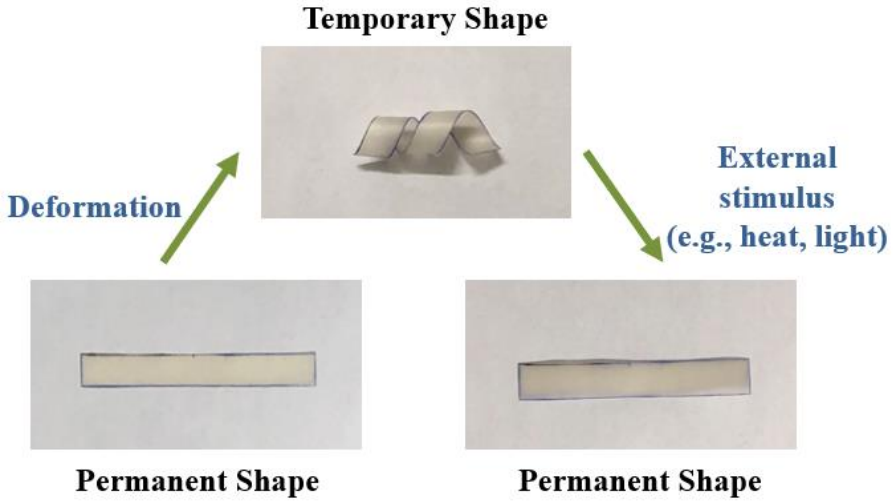

Figure 2.1 A brief illustration of the effect of SMM

SMA was discovered in the early 1900s. [3,4] Until the 1960s, the first SMA made of nickel and titanium was produced and applied by Buechler and his co-workers at the Naval Ordnance Laboratory, named Nitinol. [4–6] In the following period, it has a rapid growth due to its good properties, such as high strength, fatigue resistance, and wear resistance. [7,8] The shape memory effect of SMA is implemented by phase transition between the austenitic phase and martensitic phase in the alloy. At a relatively low temperature, the alloy stays in the martensitic phase and can be deformed into the desired temporary shape. Whereas the transition from the martensitic phase to the austenitic phase takes place when heated above the transition temperature. With the alloy completely in the martensitic phase, the alloy exhibits super elasticity that allows recovery to the original shape. [3,4] For SMA, the more common stimuli to achieve the shape memory effect are thermal, or magnetic. Moreover, SMA is still expected to have a great potential for future development in aerospace [9], automotive [10], and biomedical [3–5,9] fields.

Compared to SMA, SMP demonstrates its benefits in a number of aspects. SMP requires simpler processing conditions in terms of temperature and pressure, which leads to a lower cost. [11–17] What's more, SMP can be stretched to higher elongation (up to 600%), while SMA can only reach ~8%. [8,17] There are also more stimuli besides heat that can stimulate the SMP, such as light, PH, chemical and electrical. [15,18] These privileged properties have gradually allowed SMP to gain more attention. And various applications have been implemented in the fields of sensors, [19–22]

aerospace, [23–25] biomedical devices, [5,15,26,27] and textiles. [11,25,28] The market size of SMP has shown continuous growth over the past few decades. Till 2022, the market size of SMP has reached USD 520 million, and it is still expected to have a growth of 26.5% over the next decade due to the growing demand in various fields. [29] Moreover, being the focus of this study, more about SMP would be described below.

Properties	SMA	SMP
Processing Conditions	>1000˚C, high pressure	<200˚C, low pressure
Extent of deformation	<8%	Up to 600%
Biocompatibility	High	Low
Deformation stress (MPa)	50-200	1-3
Recovery stress (MPa)	150-300	1-3
Cost	Expensive	Cheap

Table 2.1 Comparison of properties of SMA with SMP

2.2 Shape Memory Polymer

2.2.1 Mechanism of Shape Memory Polymers

In order to enable the shape memory effect, it is necessary for SMPs to meet specific requirements in the internal structure. SMPs consist of two phases that work together and play their respective roles for the shape memory effect. One phase is the reversible phase, also can be

considered as a "switch". It is an essential element responsible for the shape transition. The other phase is a permanent phase composed of the elastic network, responsible for restoring to the permanent shape of the polymer.

Many models have been developed to illustrate the working mechanism in SMP, e.g., the thermoviscoelastic theory model [25,30] and the phase transition theory [25,31]. Hu *et al.* described a molecular structure model consisting of net-points and switches to explain the mechanism applicable to SMP in general. [32] As shown in Figure 2.2, the net-points refer to the connections that compose the crosslinking network, and the switches are reversible regions of the structure that control the shape memory process. Net-points can be induced by physical cross-linking, chemical cross-linking, complex structural entanglement, etc. [25,32] As for the switches, they are domains that allow for reversible transitions such as crystallization, glass transition, and reversible covalent bonding. [32–34]

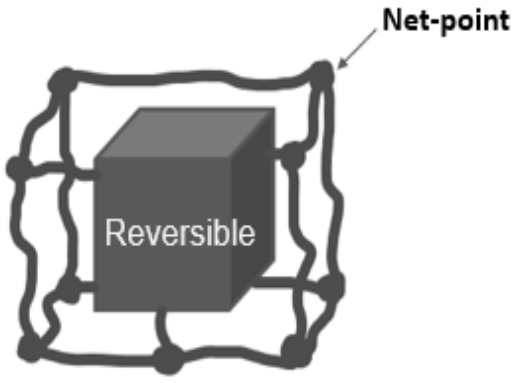

Figure 2.2 Molecular structure model of SMP

2.2.2 Categorization of Shape Memory Polymers

Over the years, numerous SMPs have been developed. SMPs utilize different combinations of ingredients, mechanisms, and stimulus. As shown in Figure 2.3, SMPs can be classified according to each feature. For instance, according to the chemical structure of the polymer, SMPs can be classified into block copolymer SMPs, crosslinked homopolymer SMPs, polymer blend SMPs, etc. Based on the various stimulus mentioned earlier for activating shape memory effect, SMPs can be categorized into heat-induced SMPs, electric-induced SMPs, light-induced SMPs, magnetic-induced SMPs, etc. In addition, SMPs can also be distinguished upon different types of net-points in the structure, which are physically crosslinked and chemically crosslinked polymers. Moreover, depending on the eventual shape memory effect shown, one-way SMPs, two-way SMPs, triple shape SMPs, and multi-shape shape memory effect can be differentiated. [35]

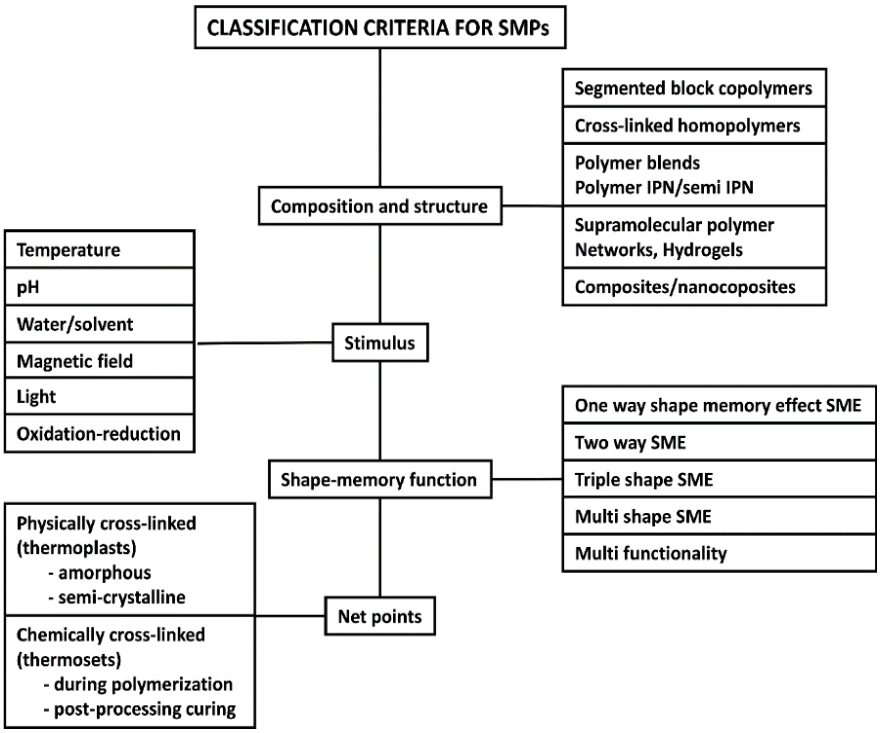

Figure 2.3 Classification criteria for SMP (Reproduced with permission from Springer Nature) [35]

2.2.2.1 Categorization by Stimulus

The most common type is normally heat-induced SMP as it can be triggered more easily. Heat-induced SMP relies mainly on phase transitions, such as crystallization and glass transition. [36] And the activation temperature of the "switch" is the corresponding phase transition temperature, that is T_g for the glass transition and T_m for the melting of crystals, respectively. For example, Li *et al.* described the shape memory effect of the maleated polyethylene (mPE)/nylon6 graft copolymer. In this study, mPE and nylon6 were melt blended in a Haake mixer at 230 ˚C for melt

blending. During the mixing process, the amine groups of nylon6 reacted with the functional groups on mPE to generate the mPE-graft-nylon6 copolymer.[37] In this shape memory system, the crystalline phase of mPE acted as the switch that allowed the transition between the two phases around the T_m of mPE. While the physical crosslinking network was constructed by the nylon domains in the copolymer structure. The results showed that the mPE-graft-nylon6 copolymer exhibited good shape memory effect.[38]

In addition to the heat-induced SMP, the electric-induced SMP is another widely used type of SMP. Distinct from other stimuli, most electric-induced SMPs are indirectly initiated by the heat generated from electricity, rather than directly by electrical stimulation to alter their shape. For instance, Cho *et al.* demonstrated the electric-active shape memory behaviour of the polyurethane (PU)/multi-walled carbon nanotube (MWCNT) composite. The soft and hard segments existing in the synthesized PU played the role of the "switch" and that of the permanent network, respectively. Cho *et al.* explained that higher loading of MWCNT led to higher electrical conductivity of the material. Thus, with certain voltages applied, it was also able to have a faster heating rate to reach the transition temperature T_g and trigger the shape memory effect. [39]

Moreover, light-activated SMP has received increasing attentions as its unique characteristics, such as the capability for remote activation. [40,41] For light-induced SMP, the activation is performed in a noticeably different way than heat-induced SMP. Lendlein *et al.*

illustrated a light-induced SMP by engrafting photosensitive cinnamic groups into a permanent polymer network. The cinnamic groups were responsible for acting as a "switch" in this SMP, having the ability to cross-link under lighting at a wavelength higher than 260 mm. The higher intense network produced under lighting allowed fixation after deformation. In contrast, the decrosslinking of the cinnamic groups occurred at wavelengths below 260 mm, which permitted the SMP to remove the barrier and free to return to its original shape. [42] In this case, this photo-reversible group was the one that led to the realization of the SME.

Lastly, a novel type of SMP has also been extensively studied recently, which is the magnetic-induced SMP. For this class of SMPs, magnetic particles are introduced for dispersion in the polymer matrix, and then heated by an alternating magnetic field to activate the shape memory effect.[43] Zhao *et al.* designed a PLA/ Fe_3O_4 SMP used as a porous bone tissue scaffold for the treatment of bone defects. In this study, the shape memory PLA/Fe_3O_4 filament was first obtained by blending 80wt% PLA and 20wt% Fe_3O_4 in the extruder, then the porous scaffold structure with desired porosity was fabricated using 3D printing. The Fe_3O_4 particles would start to move when an alternating magnetic field was applied, resulting in friction with the PLA molecules that generate the heat to activate the shape recovery. The results indicated the mechanical stability and biocompatibility of this scaffold. In addition, its shape memory effect was verified, which makes it a potential direction for further research.[44]

2.2.2.2 Categorization by Net-points

SMP can also be categorized by the type of network constructed by the net-points existing in the SMP. Two major categories are chemical crosslinking and physical crosslinking.

Chemical crosslinking is mainly composed of covalent bonding resulting from various chemical reactions. Safranski *et al.* revealed an (meth)acrylate-based SMP. The crosslinking network in this SMP was synthesized by the UV photopolymerization reaction between the mono-functional (meth)acrylate monomer and the multi-functional (meth)acrylate crosslinking agent. Therefore, this chemical network would act as the permanent phase, while the glass transition served as the reversible phase in this shape memory system. In addition, the crosslink density of this (meth)acrylate-based SMP proven to be effective in influencing the mechanical properties and the toughness.[45]

For physical crosslinking, it is made up of weaker connections, such as ionic bonds, hydrogen bonds, van der Waals force, etc.[46] For example, a novel SMP design of zinc stearate (ZnSt)/ionomer composite was presented by Weiss *et al*. In this study, sulfonated EPDM, which was a thermoplastic elastomer, was investigated as the ionomer. A large number of ions in the sulfonated EPDM developed a physical network in the SMP. Zinc stearate, as a kind of fatty salt, provided the switch for this SMP by its own melting behavior. By mixing the ionomer with varying

amount of ZnSt, SMPs with different transition temperatures and softness were obtained.[47] Compared to chemically cross-linked SMPs, physically cross-linked SMPs hold weaker cross-linked connections, which would result in relatively lower stability and durability in the network structure.

2.2.2.3 Categorization by Shape Memory Functions

According to the classification in Figure 2.3, shape memory effect typically consists of one-way shape memory effect, and two-way shape memory effect, multi-shape shape memory effect, etc. One-way shape memory effect is the most commonly used type and forms the basis for the development of materials with other shape memory functions. Its deformation process is limited to a given direction, and repeated SM cycles cannot be realized without the action of external forces. [48] One-way shape memory effect is also the intended effect of the polymer blends in this study.

Two main parts in the one-way shape memory effect are programming and recovery. As the first part, programming is responsible for assigning the designed temporary shape to the material. This involves several steps, including heating to the transition temperature, applying an external force to load the intended shape, holding, and cooling for fixing. [48,49] Recovery follows as the second part, which enables the return from the programmed temporary shape to the

permanent original shape.

Two-way shape memory effect, on the other hand, is a relatively more recent area to be explored in the field of shape memory. It has the ability to achieve reversible and repeatable shift between two shapes.[50] For instance, Chen *et al.* developed a thermal-induced SMP with two-way shape memory effect by utilizing two different layers of polyurethane. In this study, a pre-deformed active layer of PHAG5000 based shape memory polyurethane (SMPU) was glued to an undeformed PBAG600 based polyurethane substrate layer. The first shape changed from shape 1 to shape 2 is due to the gradual release of stress from the deformed SMPU during heating. As the deformed SMPU recovered its shape, a corresponding bending deformation of the polyurethane substrate occurred. The subsequent shift from shape 2 back to shape 1 occurred as a result of the bending force in the substrate. This bilayer material was validated to convert between two shapes in the range of 10-60 °C.[51]

Moreover, multi-shape shape memory effect refers to the implementation of several temporary shapes under the stimulus as compared to one-way shape memory effect that realizes only one temporary shape in the SM cycle. To briefly illustrate with three shapes, the shape variations can be summarized as permanent shape, temporary shape 1, temporary shape 2, temporary shape 1, permanent shape. Samuel *et al.* designed a PLLA/PMMA polymer blend capable of achieving triple-shape shape memory effect. This polymer blend exhibited a relatively

broad glass transition temperature. And the glass transition temperature altered accordingly whenever the stretching temperature varied. Then two temporary shapes could be memorized separately by stretching twice at gradually increasing temperatures. [52] This study offered an essential idea for the design of the multi-shape shape memory effect and revealed the potential for its further development.

2.2.3 Characterization of Shape Memory Effect

As mentioned earlier, the shape memory effect defines the typical effect that can be implemented by shape memory materials, referring to a full SM cycle in which the material switches between the original shape and the programmed shape in response to the designed stimulus. Therefore, the characterization of the shape memory effect is critical for evaluating the shape memory performance of the developed SMP.

Figure 2.4 displays a schematic of a typical one-way SM cycle for thermal-induced materials. The SM cycle can be divided into two basic processes. The process of transferring from the initial permanent shape to the temporary programmed shape is known as the programming process, while the subsequent process of returning from the temporary shape to the permanent shape is considered as the recovery process. [48,49]

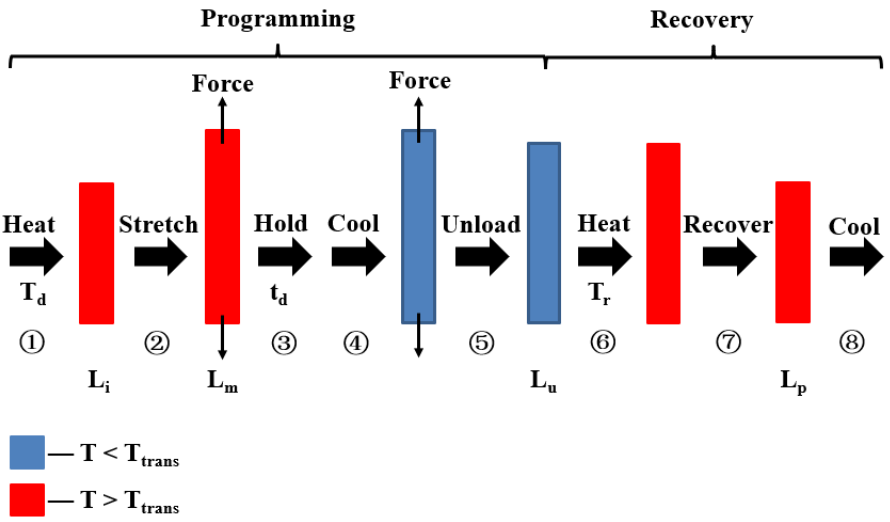

Figure 2.4 Schematic of the typical thermal-induced SM cycle

Two parameters can then be derived from the measurements taken during the SM cycle, namely fixity and recovery. Fixity (R_f), as the name suggests, is a factor that describes the ability of the polymer to maintain a temporary shape after the programming process, while recovery (R_r) reflects the ability of the polymer to recover from a temporary to a permanent shape. These two parameters will be a powerful reference when comparing the performance among different SMPs. Chemically crosslinked epoxy-based SMPs, for example, usually have excellent shape memory properties, with fixity and recovery of 95-100%. Physically crosslinked amorphous PUs, on the other hand, typically achieve fixity of 80-90%, while recovery ranges from 75% to 100%.[53]

2.3 TPU/PLA Shape Memory Polymer Blend

Environment-related issues have recently been increasingly noticed in manufacturing.[54]

Common concerns regarding polymers are pollution during the manufacturing process and degradation in nature.[54–56] Therefore, the use of biodegradable polymers is a fashionable trend to address such issues. Being a biopolymer, polylactic acid (PLA) has gained attention due to its eco-friendly and biodegradable properties.

The chemical structure of PLA is displayed in Figure 2.5(a). PLA is produced by polymerization using a bio-derived monomer, lactic acid.[55] Lactic acid is an organic acid that can be obtained directly from nature. Upon use, PLA can be hydrolyzed back to lactic acid without any toxic by-products.[54,55] Also, PLA exhibits a fairly low glass transition temperature Tg, approximately 55-65 °C.[57,58] These properties allow PLA to be used in a wide range of applications, especially in biomedical devices.[56,59] For example, Felfel *et al.* illustrated a bioabsorbable fixation device made of PLA for bone surgery. The benefit of using PLA is that a second surgery is no longer required to remove the device. This prevents a second injury to the patient. Moreover, the stiffness of PLA proved to be a good fit with cortical bone.[59]

What's more, as a semi-crystalline polymer, PLA is capable of realizing the shape memory effect on its own. The crystalline region and highly entangled polymer chains act as the permanent phase for shape recovery.[60,61] The amorphous region of PLA, on the other hand, represents the reversible phase that can be used to assist in fixing temporary shapes by altering the mobility of the polymer chains through the glass transition.[57,58,61] Despite these strengths, weaknesses in the

mechanical properties of PLA remain evident, such as brittleness, low elongation, and poor toughness.[55,62,63] These have somewhat restricted the development of PLA in many aspects, especially in shape memory.

Blending with thermoplastic polyurethane (TPU) is considered to be an efficient approach to tackle this problem. Blending denotes the process of combining two or more different polymers to develop materials with new properties.[64] To begin with, a brief distinction needs to be made between polyurethane (PU) and thermoplastic polyurethane (TPU). PUs are primarily thermosets, which means that an irreversible curing reaction would occur upon heating.[65] On the other hand, TPU defines as a type of thermoplastic elastomer as well as a block copolymer without crosslinks in the structure. As displayed in Figure 2.5 (b), it consists of two alternating segments, the soft segment and the hard segment. The amorphous soft segment provides the resilience of the material.[66,67] And the hard segment allows the formation of a physical networking through hydrogen bonding, which brings toughness to the material.[66–69] These attributes give TPU several favorable properties, including durability, elasticity, toughness as well as biocompatibility.[66,69,70] What's more, the TPU-based SMP is therefore one of the most desirable types of SMPs with a recognized potential for growth. Accordingly, the mechanical properties could be significantly optimized by blending PLA with TPU.

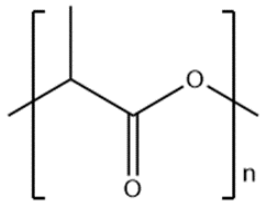

(a)

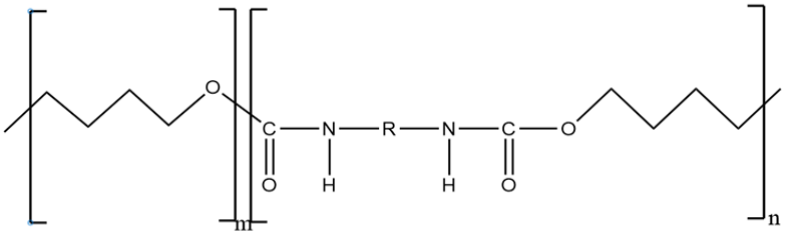

(b)

Figure 2.5 Chemical structure of: (a) PLA (b) ether-based TPU

Similarly, two phases are present in the TPU/PLA polymer blend system to realize the shape memory effect. The glass transition of PLA serves as the reversible phase in the material which is the trigger to activate the effect. As a result, the glass transition temperature Tg is considered a key parameter in the study. The physical networking constructed by the hard segment in TPU, on the other hand, represents the permanent phase intended to maintain the permanent shape of the material and provide restoring force. Such polymer blend exhibit great potential for many applications, especially in biomedical applications. [71–73]

2.4 Parameters Affecting the Properties of TPU/PLA Polymer Blend

Ever since the development of the TPU/PLA polymer blend, a number of parameters that may contribute to its properties, including mechanical properties, shape memory properties, etc., have been investigated by researchers. The studied parameters are related to material composition or processing condition. Furthermore, these studies could provide a foundation and valuable guidance for further research related to the development of the TPU/PLA polymer blend.

2.4.1 Material Parameters

To develop and study a certain type of material, one of the primary concerns is its basic components for fabrication, including their selection, ratios, etc. These considerations can determine the fundamental structure and properties of the material to a certain degree. Therefore, some studies have started with a basic exploration of the relationship between the proportion of the two ingredient polymers and the corresponding exhibited shape memory properties of TPU/PLA shape memory polymer.

Jing *et al.* investigated the properties and morphology of TPU/PLA polymer blends with PLA contents of 60%, 70%, 80%, and 90%, respectively. Firstly, the morphology of the polymer blends was illustrated by SEM, micro-raman spectroscopy and DSC tests. That is, the two components, TPU and PLA, were immiscible with each other. And there were two phases present

in the blend rather than a single phase. And the stress-strain tests indicated that the tensile elongation and toughness of the material were both enhanced by the addition of TPU to PLA. Moreover, preliminary shape memory effect analysis and characterization of selected samples were performed and repeated cyclic tests were carried out. It was worth noting that room temperature was used here as the pre-deformation temperature, while 70 °C was selected as the recovery temperature. Under this condition, the blends exhibited fair shape memory properties, achieved fixity in the range of 70% to 80% and recovery above 90%. [74]

These previous studies provided a good description of the basic structure and properties of TPU/PLA polymer blends and introduced the fundamental shape memory situation of the hybrid system. However, there are still a number of parts lacking discussion, especially those polymer blends with TPU as the dominant component, and variations in the internal behaviors due to changing compositions, such as crystallization behaviors. Therefore, a better and more in-depth understanding of the influence of the components on the internal behavior is worthwhile and would benefit the further development of the TPU/PLA polymer blend system.

Furthermore, the addition of fillers is generally a common and effective method for polymer modification to improve certain existing properties, to achieve changes in structural morphology or to introduce new features. In the case of TPU/PLA polymer blends the purpose of modification typically is to improve the mechanical properties, thermal conductivity, electrical conductivity, as

well as the shape memory properties. A number of fillers have been utilized to modify TPU/PLA polymer composite in order to achieve diverse properties, such as carbon nanotubes (CNTs), multi-walled carbon nanotubes (MWCNTs), carbon black (CB), graphene oxide, and so on. [39,75–78]

A previous study conducted by Qi *et al.* demonstrated TPU/PLA polymer composites filled with carbon black (CB). Samples used in the experiments had a TPU/PLA composition of 30/70 and a CB content of 0 to 8 phr. It was proved that the addition of CB transformed the interior of the polymer composite from an island structure to a co-continuous structure. [78–80] As a result of the new inner structure appeared in the polymer composite, better shape memory performance was obtained, especially in the recovery. Furthermore, the electrical conductivity of the material was obviously improved as well. [78]

Although several fillers have been investigated, research regarding the effect of hexagonal boron nitride (h-BN) on the shape memory properties of TPU/PLA polymer blends remains a gap. Hexagonal boron nitride (h-BN) is a type of ceramic material with a two-dimensional layered structure similar to graphene. [81,82] The microstructure of BN is shown in Figure 2.6. B and N atoms are connected by strong inter-layer covalent bonds, while the layers are bound by relatively weak Vander Waals bonds. [82–84] It exhibits excellent performance in many aspects such as mechanical properties, electrical insulation, thermal stability, and thermal conductivity, etc. [83,85–87] Thus, it finds a wide range of applications in electronic appliances, lubrication, insulation, and as a filler

in the manufacture of composite materials. [82–86]

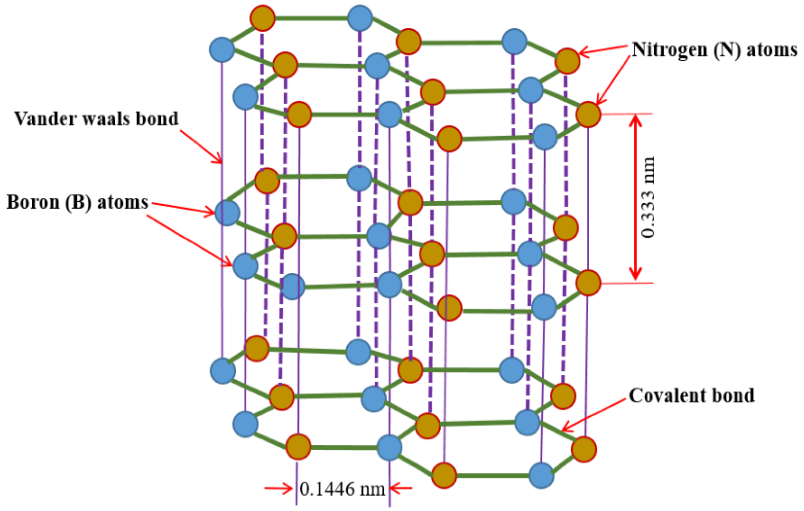

Figure 2.6 Microstructure of hexagonal boron nitride (h–BN) (Reproduced with permission from Elsevier)[84]

Previous studies regarding h-BN primarily focused on its effect on thermal conductivity. For example, Li *et al.* investigated the impact of particle size of h-BN on the thermal conductivity of polypropylene (PP)/h-BN used in 3D printing. The 3D printing technique selected for this study was fused filament fabrication (FFF). Due to the characteristic of this method, the filler would be aligned during the printing process. Polymer composites, which contain h-BN with different particle sizes of 4 μm, 15 μm and 27 μm, were then prepared. The results indicated that a larger particle size of h-BN gave a better alignment in the printing direction and consequently a higher thermal conductivity. [88]

The role of h-BN in shape memory properties deserves more exploration and anticipation. For TPU/PLA polymer blend, the presence of N atoms in the microstructure of h-BN fulfills the basic requirement for hydrogen bonding with TPU. Consequently, it could be assumed that the addition of h-BN may affect the physical network density in polymer composites. Moreover, the high thermal conductivity of h-BN also favors the recovery of such thermally induced SMPs. Thus, research on TPU/PLA/h-BN polymer composites is needed.

2.4.2 Processing Parameters

Besides considering the parameters related to the composition of the material, additional parameters present of the processing deserve concern as well. A study conducted by Zhao *et al.* described a solid hot stretching method, where the polymer blends were processed by stretching through a convergence die at 90 °C with a certain stretch ratio after compounding, to manufacture TPU/PLA polymer blends with higher internal orientation for biomedical research. The results revealed that this method improved the mechanical properties of the material, such as modulus and strength. The corresponding crystallinity was also promoted due to the occurrence of stress-induced crystallization during the process. [89] And this study could be informative when considering the effects of similar conditions related to stretching in processes of manufacturing or testing. And a section of this article presents a related study in shape memory with this thinking.

What's more, the cooling process of non-isothermal crystallization is known as an important determinant of the properties of semi-crystalline polymers, such as crystallization and tensile strength.[90,91] And a number of studies on various semi-crystalline polymers have demonstrated this. Take polypropylene as an example first, the impact of cooling rate on its crystallization behavior was illustrated in a study by Hu *et al.* Polypropylene samples were chilled at 18 different rates for crystallization. The results showed that both the crystallization temperature and the crystallinity decreased as the cooling rate increased. In addition, as shown in Figure 2.7, a model was developed to describe the relationship between the crystallinity and the cooling rate. The obtained graph indicated that the crystallinity decreased sharply at the beginning, while the drop rate of the crystallinity would flatten out when the cooling rate got sufficiently high. [91]

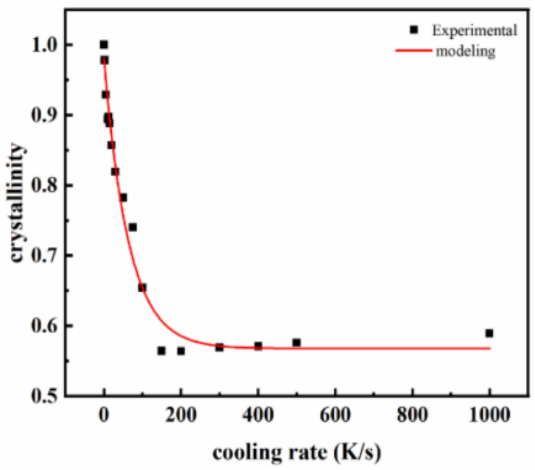

Figure 2.7 A model to illustrate the relationship between the crystallinity and the cooling rate of polypropylene (Reproduced with permission from MDPI) [91]

As a common semi-crystalline polymer, the influence of cooling rate in materials containing PLA has also been investigated. Hu *et al.* investigated the effect of cooling rate on the crystallization of polylactic acid (PLA)/polyethylene glycol (PEG) polymer blends. In this study, three proportions of polymer blends, i.e., 90/10, 80/20, and 70/30 PLA/PEG, were cooled at different cooling rates from 185 °C to -25 °C. And the crystallinity of the polymer blends was improved by using slower cooling rates. More specifically, since both PLA and PEG belong to the group of semi-crystalline polymers, a lower cooling rate enhanced the crystallinity of both components. Eventually, 5°C/min or less was considered to be the appropriate cooling rate to maximize the crystallinity of the PLA/PEG polymer blends.[92] In addition, the effect of PLA crystallization on shape memory effect was investigated in the study of Cunha *et al*. In that study, PLA samples with different degrees of crystallinity were prepared by different heat treatments and then tested for shape memory properties. The results indicated that crystallization could promote the shape memory effect of PLA.[93] Therefore, the impact of crystallinity of PLA governed cooling rate is also a point of concern for the TPU/PLA shape memory polymer blends.

Besides the fabrication process, many of the parameters in the SM test cycle are supposed to be considered as well. As an essential analytical tool for shape memory polymers, the SM cycle provides a series of steps to assess shape memory capabilities. However, the relevance of some conditions in performing these steps has been somewhat neglected by researchers. Referring to the

steps of the SM cycle in Figure 2.4, these constraints include temperatures (deformation/recovery), holding time in stretching, deformation rate, applied strain, and so on.

As the TPU/PLA shape memory system is thermally activated, the temperature-related factors in the SM testing cycle have become the first concern. Several previous studies have described and compared the effect of processing temperatures, including the pre-deformation and the recovery temperature, on shape memory properties.[31,94] For instance, Lai *et al.* investigated the shape memory effect of TPU/PLA polymer blends at three predeformation temperatures of 25, 80, and 120 °C as well as various recovery temperatures. In this study, 30/70 and 50/50 TPU/PLA polymer blends were prepared. At a constant recovery temperature of 80 °C, the fixity increased with increasing deformation temperature, while the recovery decreased oppositely. Moreover, by introducing a factor that multiplies the fixity and recovery, it was indicated that the shape memory properties improve with increasing recovery temperature at a certain predeformation temperature.[94]

Although several conditions, especially temperature-related ones, have been investigated, numerous processes, such as the stretching at the deformation temperature to achieve the temporary shape, and their correlation factors are still under discussion. This suggests the need for more exploration of the activities that occur during the SM testing cycle. In response to this situation, a part of this study would target the exploration of a previously neglected factor in the

SM cycle and provide a deeper understanding of its role and the associated effects it brings on shape memory performance.

Chapter 3. Experimental

3.1 Materials and Design

The research highlighted two key polymer components: polylactic acid (PLA) and thermoplastic polyurethane (TPU). PLA (3052D) was procured from NatureWorks LLC, while TPU (2103-70A) was sourced from Lubrizol Engineered Polymers. PLA boasts a specific gravity of 1.24 g/cm^3, a tensile elongation of 3.5%, a tensile yield strength of 62 MPa, as well as a glass transition temperature (Tg) between 55 and 60 ˚C. Whereas TPU exhibits a specific gravity of 1.06 g/cm^3 and a glass transition temperature (Tg) of -69 ˚C.

The filler material employed in the study for the polymers was hexagonal boron nitride (h-BN). The h-BN used here in was h-BN (AC6041) sourced from Momentive Performance Materials, characterized by a particle size is 5 μm.

3.2 Preparation of TPU/PLA Blends

The PLA and TPU pellets underwent an initial drying process under vacuum conditions at 80˚C for 4 hours to remove any moisture content. [94] Following this, samples of varying compositions were accurately weighed based on the specifications outlined in Table 3.1. [95]

Sample Designation	TPU (wt%)	PLA (wt%)
PLA	0	100
50/50 TPU/PLA	50	50
65/35 TPU/PLA	65	35
80/20 TPU/PLA	80	20
TPU	100	0

Table 3.1 Compositions of samples prepared in this research

The sequential procedures to prepare the SMP samples is shown in the schematic illustrated in Figure 3.1. Following mechanical mixing of the weighed TPU and PLA pellets in the designed proportions with a total weight of 4 g per batch, they were introduced into a twin-screw compounder (HAAKE™ MiniCTW, Thermo Scientific) for melt compounding at 180˚C and 50 rpm. Subsequently, strip samples, depicted in Figure 3.2(a), were obtained through extrusion. To fabricate thin film samples, as illustrated in Figure 3.2(b), these extrudates were pelletized and fed into the compression molding machine for 10 mins at 180 ˚C in a circular mold with a diameter of 115 mm and a thickness of 0.25 mm.[94]

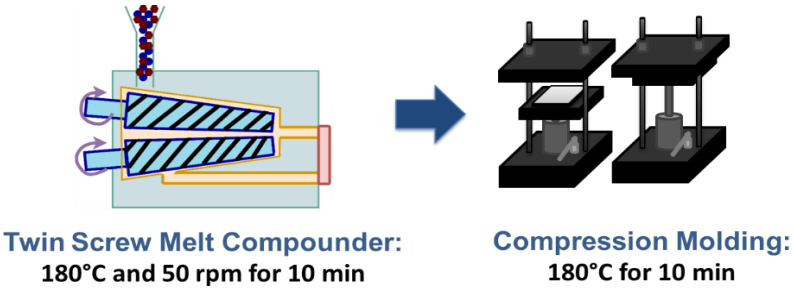

Figure 3.1 Schematics to illustrate the sequential procedures for sample preparation

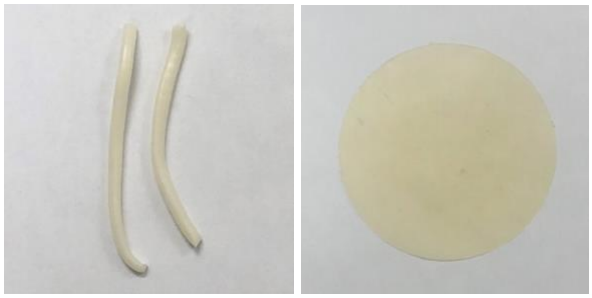

(a) (b)

Figure 3.2 Schematic view of samples with different shapes (a) strip (b) film

Finally, the final compression-molded SMP blend films were cooled. All chapters except Chapter 6 used the water cooling machine presented in Figure 3.3 for sample cooling, which consists of two panels with cooling water flowing through the sides. While three distinct cooling schemes were examined in Chapter 6, more detailed descriptions will be included in Chapter 6. Samples were further cut into specific shapes to meet some of the characterization needs. For example, for the characterization of the shape memory effect, specimens are shaped into small rectangular pieces of 5 mm x 50 mm x 0.25 mm.

Figure 3.3 Machine for water cooling

3.3 Characterization and Measurement

3.3.1 Scanning Electron Microscopy (SEM)

Scanning electron microscopy (SEM) refers to an electron microscope extensively utilized across various disciplines for morphological and microstructural analyses. Its fundamental principle involves emitting a high-energy electron beam to scan the surface of a sample and gather the resulting signal intensity. [96,97] This collected signal enables the visualization and capture of the sample's corresponding microstructure. The SEM-generated images offer higher resolution when compared to conventional microscopes like optical microscopes, facilitating detailed analysis and characterization of the material's phase morphology. [96–98]

In this study, the SEM (FEI Company Quanta 3D FEG) was utilized to assess the morphology of TPU/PLA polymer blends. All fabricated samples were cryo-fractured to expose their cross-sections and subsequently sputter-coated by a thin layer of gold before analyzed by SEM. [98]

3.3.2 Differential Scanning Calorimetry (DSC)

Differential Scanning Calorimetry (DSC) serves as an invaluable tool for investigating the thermal characteristics of polymers. As its name suggests, DSC gauges these properties by

detecting the differential heat transfers between the pan containing the sample and a reference empty pan during the heating and/or cooling cycles.[99] This resulting thermograph of the sample being tested enables the determination of various thermal characteristics of the sample. These include but are not limited to crystallization temperature, degree of crystallinity, glass transition temperature, and melting temperature.

In this thesis research, DSC (TA Instruments, 250) was employed to scrutinize characteristic temperatures and degree of crystallinity of TPU/PLA polymer blends. It must be noted that the maximum temperature of the heating cycle has to exceed the melting temperature of PLA (145-160˚C) but remain below the decomposition temperature of TPU (~270°C) and PLA (290–380°C) [100]. Thus, the chosen temperature range for the testing process spanned from 0 °C to 200 °C to ensure comprehensive assessment while maintaining the integrity of the materials under examination.

Tzero aluminum pans (i.e., temperature range: -180 to 600°C) were employed to contain the samples. Each test comprised three temperature ramps under an inert nitrogen environment. This initial heating phase from 0 to 200°C, succeeded by a cooling phase from 200 to 0°C, and a second heating phase from 0 to 200°C. The heating and cooling rates for all tests were consistently set to 10˚C/min.

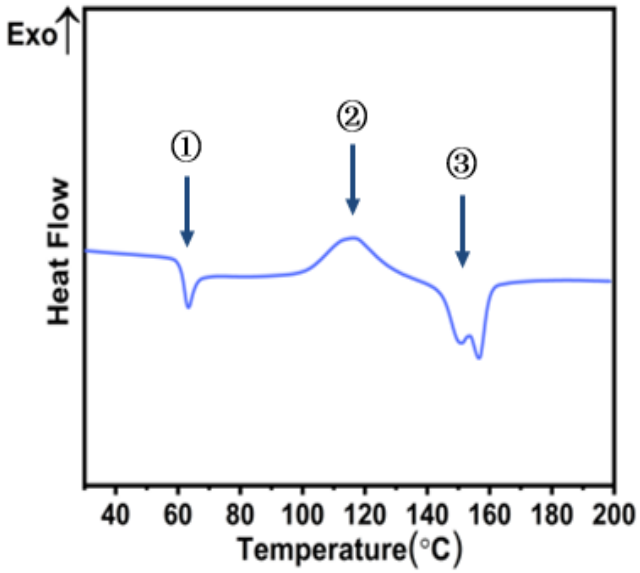

Figure 3.4 A representative heating curve of the DSC thermogram for TPU/PLA polymer blends

The corresponding DSC thermograms illustrate the characteristic transitions of TPU/PLA polymer blends that could be obtained from the tests. Due to the continuous curves plotted in DSC analysis, only one representative curve for each sample from the tests could be illustrated per DSC thermogram, even if there are more than three repetitions of the experiment. In Figure 3.4, a representative heating curve of the DSC thermogram was presented. At approximately 65˚C, label 1 marked the glass transition of PLA, a pivotal phase change crucial for the achieving the shape memory effect. Label 2, observed around 120 ˚C, denoted the cold crystallization of PLA, while label 3 indicated the melting peak of PLA, occurring at approximately 150 ˚C.

Following the analysis of these transitions depicted on DSC thermograms, crucial data, including the melting temperature, glass transition temperature, as well as enthalpy of crystal

melting or crystallization, was extracted. Moreover, the degree of crystallinity of the polymer components can be calculated utilizing Equation (3.1):

$$X_c = \frac{\Delta H_m - \Delta H_{cc}}{\frac{M_1}{M_1 + M_2} \times \Delta H_m^o} \tag{3.1}$$

where M_1 is the mass of PLA; M_2 is the mass of TPU; ΔH_m is the melting enthalpy of PLA; ΔH_{cc} is the cold crystallization enthalpy (J/g) of PLA; and ΔH^o_m is the enthalpy of 100% crystallized PLA (93.7 J/g).[101]

3.3.3 Mechanical Tests

The utilization of materials relies significantly on their fundamental properties. Therefore, relevant mechanical tests, such as the stress relaxation test as well as part of the shape memory effect test, were conducted on all samples by using the rheometer (Discovery HR-3, TA Instruments). While traditionally used for analyzing the rheological properties of fluids like polymer melt and suspensions,[102] the rheometer also offers a DMA (tensile) module specifically designed for conducting tensile tests under various conditions. This mode includes a range of procedures such as stress control, strain control, temperature ramping.

Stress relaxation is a common phenomenon observed in polymers, arising when polymer chains possess a certain degree of freedom and mobility. When external forces are applied, these

chains tend to disentangle and reposition themselves in alignment with the direction of the applied forces, thereby reducing the residual stresses stored within them. A schematic of the stress relaxation in this study is illustrated in Figure 3.5. As the sample is stretched to 100% strain and maintained at a constant strain, stress relaxation occurs in the sample and results in a decrease in stress. Similar to DSC tests, each plot displays only one representative curve for each sample, even if tests would be repeated over three times.

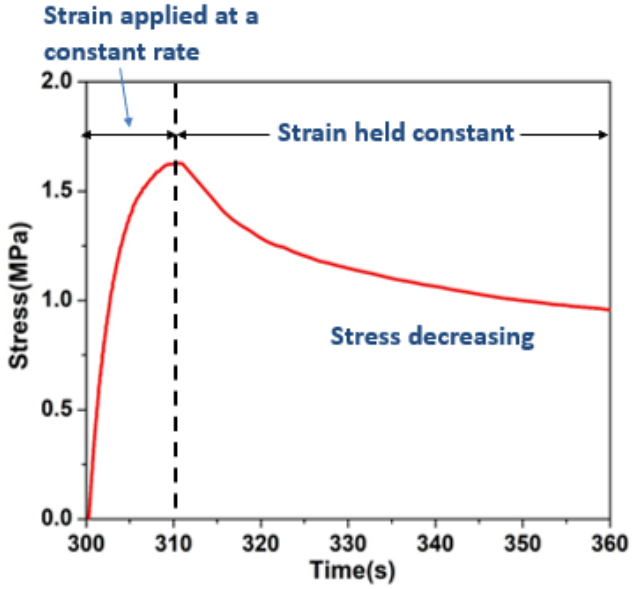

Figure 3.5 Illustration of stress relaxation under a constant strain

3.3.4 Shape Memory Properties

In Chapter 2, the evaluation of shape memory performance involves a cycling test comprising programming and recovery phases. As TPU/PLA polymer blends have been

demonstrated to achieve optimal shape memory properties when both the predeformation and recovery temperatures were set at 80 ˚C, both temperatures were thus set at 80 ˚C in this study.[94] The schematic representation in Figure 2.4 illustrates the steps involved in the shape memory cycle, which are detailed below:

STEP 1. Measure the initial permanent length L_i and heat the sample at the deformation temperature (T_d) of 80˚C for 5 minutes.

STEP 2. Stretch the sample to 100% strain at a rate of 1mm/s under 80 ˚C. Record the maximum length L_m.

STEP 3. Hold the sample with external force for specified durations (t_d) (i.e., 0 min, 1 min, 2 min, 4 min, and 6 min).

STEP 4. Cool the sample to room temperature (i.e., 20˚C) to stabilize the temporary programmed shape.

STEP 5. Remove the applied force from the sample. Allow 5 minutes for finalizing the shape and record the temporary length (L_u).

STEP 6. Reheat the sample to the recovery temperature (T_r) of 80˚C by submerging it in a hot water bath.

STEP 7. Wait for 5 minutes to allow the fully recovery of the shape. Record the recovered permanent length (L_p).

STEP 8. Cool the sample back to room temperature (i.e., 20˚C).

The step-by-step description of the shape memory cycle involves recording the sample length at each stage. These recorded lengths are instrumental in computing two key parameters - fixity (R_f) and recovery (R_r), previously described. The formulas for these parameters are presented as follows:

$$R_f = \frac{\varepsilon_u}{\varepsilon_m} = \frac{L_u}{L_m} \tag{3.2}$$

$$R_r = \frac{(\varepsilon_m - \varepsilon_p)}{\varepsilon_m} = \frac{L_m - L_p}{L_m - L_i} \tag{3.3}$$

where L_i is the initial permanent length; L_m represents the stretched maximum length; L_u is the temporary length; L_p is the Recovered permanent length. ε_m, ε_u, ε_p are the corresponding stretched strain, temporary strain and recovered strain, respectively.

Chapter 4. Fabrication and Characterization of TPU/PLA Polymer Blends with Various Compositions

4.1 Introduction

This study delves into the fabrication and characterization of TPU/PLA shape memory polymer blends with various compositions. TPU is chosen as the matrix and PLA as the dispersed phase in this investigation to enhance the material's elasticity.

In the initial phase of this study, the focus lies on investigating the effects of material composition on the material structure (e.g., degree of crystallinity) and thereby the material properties (e.g., the residual stress, fixity, and recovery) of the TPU/PLA polymer blends. This chapter aims to elucidate the mechanism by delineating the roles of TPU and PLA within the polymer blends.

The findings reveal that TPU is responsible for storing internal stress crucial for recovery, whereas PLA contributes to temporarily fixing the shape by its rigidity and glass transition. There is a trade-off between the fixity and recovery as PLA content increases in the blend, ultimately resulting in increased fixity and decreased recovery. The 65/35 TPU/PLA polymer blend demonstrates the overall best shape memory performance. What's more , it is believed that both

the residual stress and the degree of crystallinity significantly impact the shape memory properties of the blend.

4.2 Experimental

Polymer blends using TPU as the base and PLA as the dispersed phase were fabricated for investigation in this study. As described in Chapter 3, these blends were prepared following the compositions detailed in Table 3.1, ranging from 0 to 50% PLA content. They were denoted accordingly: 50/50 TPU/PLA, 65/35 TPU/PLA, and 80/20 TPU/PLA together with neat TPU and PLA.

To characterize the residual stress and the shape memory effect, all samples were cut into rectangle pieces measuring 5 mm x 50 mm x 0.25mm. For DSC characterization, small pieces of samples weighing approximately 5 mg were cut from the molded samples and utilized. Furthermore, in this chapter, the holding time after stretching at the transition temperature is consistently set to 1 minute. At least three samples of the same type were examined for each characterization testing to ensure the repeatability of the data. More details regarding the experimental procedures are described in Chapter 3.

4.3 Results and Discussion

4.3.1 Morphology

To assess the dispersion and miscibility of TPU and PLA components in the samples after blending, SEM tests were performed for each composition. The SEM micrographs are depicted in Figure 4.1, showcasing the morphology of the 50/50 TPU/PLA, 65/35 TPU/PLA, and 80/20 TPU/PLA samples in Figure 4.1 (a), (b), and (c), respectively.

In Figure 4.1(a), distinct phases are visibly evident, showing a uniform distribution of tow phases forming a co-continuous structure due to the equal proportions of both components. In Figure 4.1(b), the PLA phase no maintain continuity but rather appears as dispersed droplets within the TPU matrix. In the case of 80/20 TPU/PLA sample depicted in Fig. 4.1(c), the PLA phase forms even smaller dispersed droplets within the TPU matrix due to the reduced PLA content.

Overall, the SEM micrographs reveal the immiscibility of TPU and PLA in the polymer blends. Typically, the TPU phase, which is the major phase, acts as the matrix, while the PLA phase exists as dispersed droplets within the matrix.[74] This scenario is slightly different for the 50/50 TPU/PLA sample, where the internal structure shows greater continuity. Morphological characterization via these images provides a visual representation of the microstructure within the samples, offering insights for subsequent characterization and analysis.

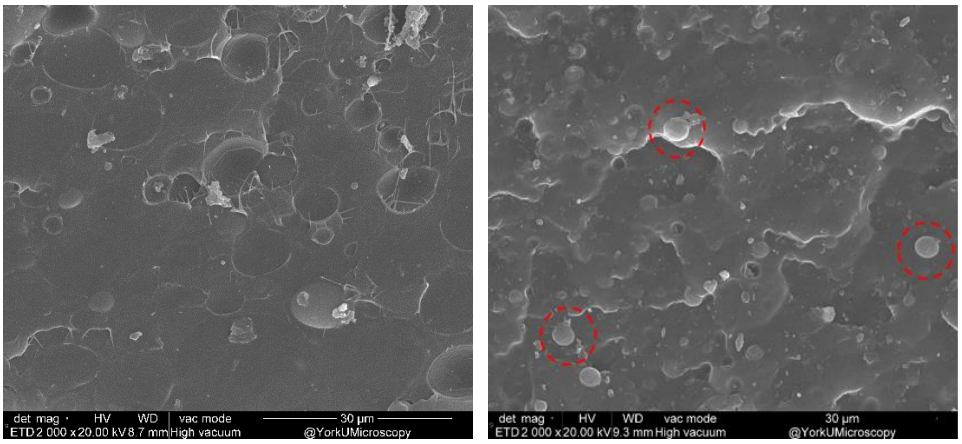

(a) (b)

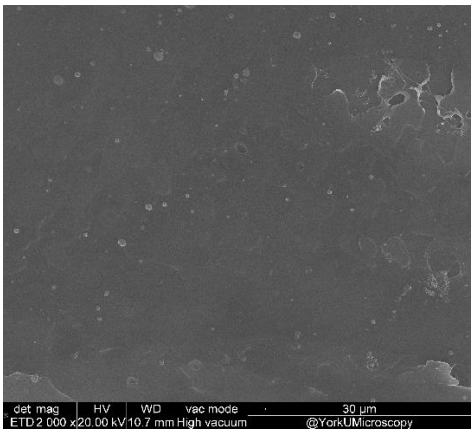

(c)

Figure 4.1 SEM micrographs of the cross-sections (note: magnification of 2000×) of (a) 50/50 TPU/PLA (b) 65/35 TPU/PLA (c) 80/20 TPU/PLA polymer blends. (Note: dispersed PLA phases are cirled in (b) as examples)

4.3.2 Stress Relaxation Tests

In this study, when the T_g of PLA marks its transition from a glassy state to a rubbery state, allowing increased mobility of its polymer chains. Whereas, TPU remains in the rubbery state as

it owns a T_g lower than the room temperature. Consequently, these conditions set the stage for stress relaxation within the TPU/PLA polymer blends.

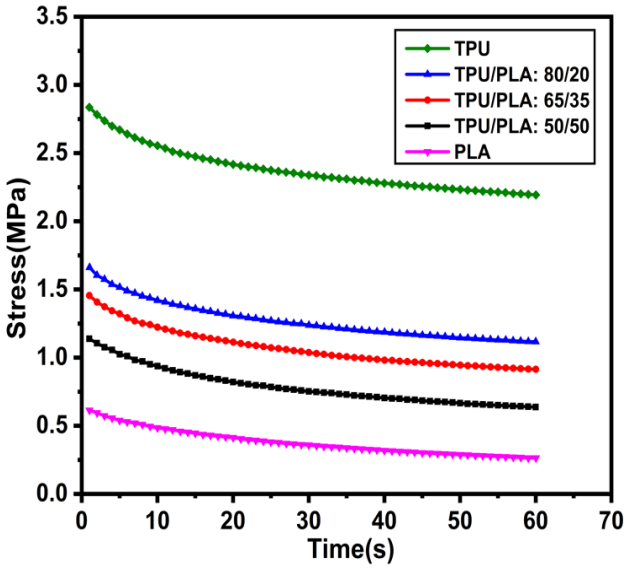

Figure 4.2 Stress Relaxation for polymer blends with various compositions

As depicted in Figure 4.2, samples across all compositions displayed varying degrees of stress relaxation subsequent to being held at the transition temperature for one minute. Notably, the physical network within TPU demands a higher stress level to achieve a 100% strain compared to PLA. Consequently, as the TPU content increases in the samples, it can be observed by the final residual stress increases. Table 4.1 summarizes the values of the initial and final residual stresses for samples with different compositions upon stress relaxation. A consistent relaxation pattern can be observed across all samples. Correspondingly, both the final stresses exhibit an ascending trend

in samples with higher TPU content.

PLA Content [%]	Initial Stress [MPa]	Final Stress [MPa]
0	2.84	2.19
20	1.66	1.12
35	1.45	0.91
50	1.14	0.64
100	0.61	0.26

Table 4.1 Initial and final stresses for samples of various compositions due to stress relaxation

4.3.3 Crystallization Behaviors Characterization

The analysis of differences in crystallization behaviors serves as an insightful tool for understanding variations in internal structure in different samples. Within TPU/PLA polymer blends, the PLA phase is recognized as the main phase capable of forming crystals, while the TPU phase remains mostly amorphous. Consequently, the degree of crystallinity of the samples is intricately linked to their PLA contents.

In polymer blends, two primary crystallization processes are typically observed. The first involves the melt crystallization of the polymer during the cooling process to solidify the molded

samples. The second is the additional cold crystallization observed upon reheating the sample, represented by a peak around 120 °C in the DSC thermogram. This study primarily focuses on analyzing the degree of crystallinity arising from melt crystallization. Therefore, whenever the degree of crystallinity is mentioned in this research, it specifically pertains to the aspect related to melt crystallization.

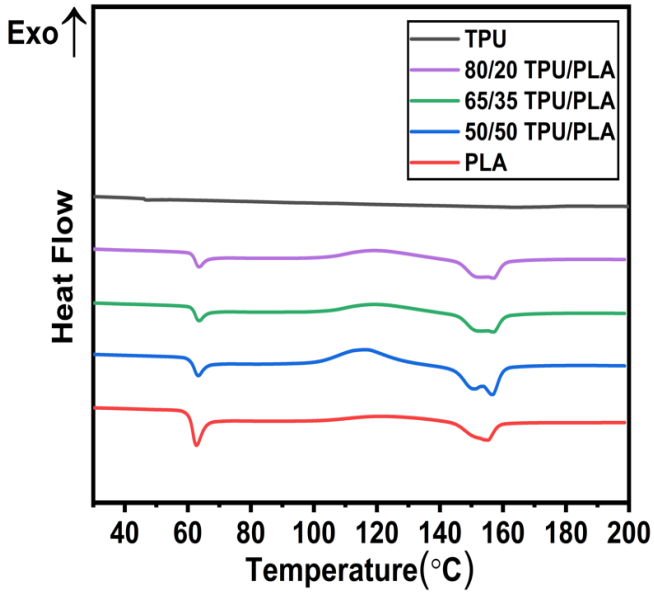

Figure 4.3 DSC thermograms of TPU/PLA polymer blends with various compositions

In Figure 4.3, the DSC plots of samples with the specified compositions are presented. As previously discussed, the thermogram of TPU appears nearly flat due to its notably low glass transition temperature and the virtual absence of crystals. However, upon the addition of PLA, distinct peaks indicative of glass transition, cold crystallization, and melting emerge on the thermograms.

The degree of crystallinity data derived from the DSC thermograms is summarized in Table 4.2. Comparatively, when blended with TPU, samples exhibit a higher degree of crystallinity than neat PLA because the presence of heterogeneous phases fostering nucleation at the initial stages of crystallization.[62] Considering the degree of crystallinity of the entire polymer blend rather than just PLA, where only a fraction of the blend contains crystalline regions, the overall degree of crystallinity of the polymer blend steadily increases as the PLA content increases.

PLA Content [%]	ΔHcc[a)] [J/g]	ΔHm[b)] [J/g]	Xc[c)] [%]	Xt[d)] [%]
0	\	\	\	\
20	5.46	6.18	3.84	0.77
35	9.86	11.37	4.60	1.61
50	14.92	18.58	7.81	3.91
100	5.90	8.49	2.76	2.76

a) Cold crystallization enthalpy; b) Melting enthalpy; c) Crystallinity; d) Crystallinity of the entire polymer blend

Table 4.2 Values of enthalpy and crystallinity

4.3.4 Shape Memory Effect Characterization

Following the examination of how material composition influences the internal structure,

residual stress, and degree of crystallinity, it is important to analyze its impact on shape memory effect. In particular, the fixity and recovery of the shape memory polymer or blend represent the key parameters to evaluate the shape memory effect of each sample. Given that PLA and TPU contribute respectively to fixity and recovery, it is anticipated that the proportion of these two components in samples will substantially influence the shape memory effect.

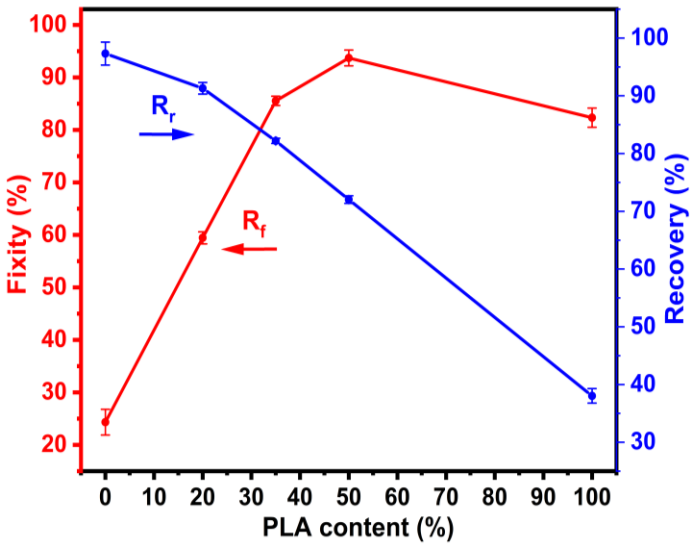

Figure 4.4 shape memory effect characterization of TPU/PLA polymer blends with various PLA content (holding time: 1min)

In this chapter, a consistent holding time of one minute under stretching was employed for the characterization purposes. Figure 4.4 illustrates the variation of fixity and recovery with increasing PLA content. Notably, the graph delineates a clear opposite trend between the two parameters. While fixity demonstrates an increase with higher PLA content, recovery exhibits a

decline.

Table 4.3 provides the average values of fixity and recovery across the samples as the PLA content varies. Spanning from 0 to 100% of PLA content, fixity ranges approximately from 25% to 82%, while recovery shows a decrease from approximately 97% to 38%.

PLA Content [%]	Fixity [%]	Recovery [%]
0	24.33 ± 2.45	97.30 ± 1.99
20	59.44 ± 1.14	91.30 ± 1.01
35	85.54 ± 0.87	82.20 ± 0.45
50	93.70 ± 1.50	72.03 ± 0.66
100	82.33 ± 1.82	38.03 ± 1.26

Table 4.3 Fixity and recovery values of TPU/PLA polymer blends with various PLA contents (holding time: 1min)

As detailed in Chapter 2, PLA possesses inherent shape memory capabilities due to the co-existence of two distinct regions in its structure: the crystalline and amorphous regions. The amorphous domain plays a pivotal role in triggering the shape transition by regulating the polymer chains' freedom, enabling fixation of the temporary shape upon cooling. Conversely, the crystalline region serves as the networking point to preserve the original shape and store energy

during the shape transition to facilitate recovery.

Building upon the shape memory mechanism inherent in PLA, the mechanism within the TPU/PLA polymer blend can be further elucidated. The inclusion of TPU can be conceptualized as introducing a new element into the permanent phase in the shape memory model, synergistically collaborating with PLA's crystalline domain to enhance recovery.

Consequently, higher PLA content leads to an increase in its amorphous region as a part of the overall polymer blend, indicating a greater number of stabilized polymer chains as their mobility diminishes during cooling. Conversely, the relative TPU content in the samples decreases, resulting in a reduced level of physical crosslinking. Stress relaxation tests also confirm a correlated reduction in the stored stress that is crucial for supporting recovery. While the addition of TPU marginally promotes PLA crystallization, its impact on the overall shape memory performance of the polymer blend is almost negligible compared to the significance of adjusting the TPU-to-PLA ratio in the blend.

4.4 Conclusion

This chapter reports the investigation on how the composition of polymer components affects the internal structure, and consequently, the shape memory properties of TPU/PLA polymer blends. Through the fabrication of samples with varying TPU/PLA ratios (50/50, 65/35, and 80/20),

an in-depth analysis was conducted, focusing on internal residual stress, crystallization behaviours, and shape memory effects.

The findings indicated that as TPU content increased, the residual stress within the sample after stretching also increased. TPU's role as the primary contributor to the physical cross-linking network led to heightened stress storage. Conversely, an elevated PLA content resulted in a slight improvement in degree of crystallinity after cooling, augmenting the overall amorphous region of PLA within the polymer blend. The stored residual stress acted as the driving force for recovery, while the amorphous region of PLA exhibited an opposing role. These internal structural characteristics directly correlated to the shape memory properties of the samples, culminating in higher fixity and lower recovery for polymer blends with a higher fraction of PLA.

In summary, both the crystalline region of PLA as well as TPU contribute to recovery, while the amorphous region of PLA aids in strengthening fixation. As an initial exploration of the TPU/PLA shape memory system, this chapter consolidated the underlying mechanisms among the primary factors influencing shape memory performance.

Chapter 5. Effect of Holding Time on Shape Memory Effect

5.1 Introduction

The analysis in Chapter IV unveiled specific internal structural attributes directly linked to the shape memory performance of the polymer blends. In addition to the blend composition, several other conditions influencing the microstucturewithin the polymer blend were explored as potential governing factors affecting the shape memory performance. Many constraints within the shape memory test cycle were considered initially. Consequently, this chapter focuses on demonstrating the significance of Step 3 in the shape memory test cycle, which involves holding the stretched material at the deformation temperature.

Various polymer blends made of different compositions were characterized at different holding times (i.e., 0, 1, 2, 4 and 6 minutes). Experimental results revealed that an increase in holding time led to a decrease in internal stored stress, attributed to the stress relaxation effect. Concurrently, the samples exhibited enhanced degree of crystallinity. Consequently, the holding time notably impacted the shape memory properties, particularly resulting in a significant decrease in recovery. This underscores the importance of considering holding time during stretching in tuning shape memory performance of a TPU/PLA polymer blend.

5.2 Experimental

This chapter aligns with the methodology established in Chapter 3 for sample preparation, focusing on fabricating samples with TPU/PLA ratios of 50/50, 65/35, 80/20, as well as pure TPU and PLA samples. The detailed process of fabricating and characterizing these samples is elaborated upon in earlier section of Chapter 3.

Furthermore, to investigate the impact of holding time of fabricated samples at the specified deformation temperature shape memory test on their structures and shape memory properties, this chapter adopts specific time intervals for investigation. The selected durations for study are 0, 1, 2, 4 and 6 minutes. For instance, the 2-minute holding time denotes maintaining an external tensile force for two minutes after the sample reaches 100% strain before the cooling process begins. Table 5.1 presents the configurations for the samples and their corresponding holding times in this study. Subsequently, experiments are conducted in accordance with these conditions. The characterization methods employed in this study, encompassing the assessment of mechanical properties, thermal behaviors, and shape memory properties, remained largely consistent.

Sample Designation	TPU (wt%)	Holding Times (min)
PLA	0	0, 1, 2, 4, 6
50/50 TPU/PLA	50	0, 1, 2, 4, 6
65/35 TPU/PLA	65	0, 1, 2, 4, 6
80/20 TPU/PLA	80	0, 1, 2, 4, 6
TPU	100	0, 1, 2, 4, 6

Table 5.1 Sample compositions and holding time during programming of samples

5.3 Results and Discussion

5.3.1 Stress Relaxation Tests

To evaluate the impact of the holding time on the internal stresses accumulated within the samples, stress relaxation tests were conducted. Despite the focus on different holding periods, the stress relaxation process followed a consistent 6-minute holding time to gather data points on the curve for each holding time.

Figure 5.2 showcases the tensile stress curves for samples fabricated at various compositions, with vertical dashed lines marking corresponding holding times for data collection. In Chapter IV, similar curves were presented for these samples held for 1 minute during stretching. Consistently, higher TPU content correlated with elevated internal stress levels. Extending the holding time resulted in a continuous decline in stress levels. Notably, all curves exhibited a similar decreasing

trend. Initially, there was a steep drop during the first one minute, followed by a gradual flattening as the holding time increased, indicating a less significant stress relaxation in the later stages. Based on the data presented in Table 5.2, there were a notable 20-50% decrease in stress after a 1-minute holding in tension. However, the reduction in stress was less than 10% from 4 minutes to 6 minutes of holding, indicating a diminished rate of stress relaxation as the holding time extended.

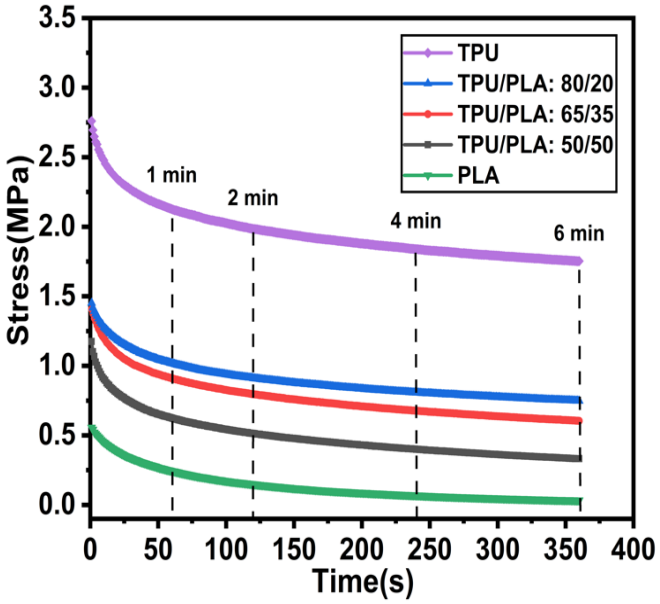

Figure 5.1 Stress Relaxation for polymer blends with varying holding times under tension

The higher content of TPU within the polymer blends provides the physical network to act as significant 'stress depositor', contributing to elevated initial stresses. Under the influence of heat and applied tension, the polymer chains progressively untangle and shift in the specified direction, initiating stress relaxation. Initially, a rapid decline in stress occurs, attributed to a substantial

transformation in chain alignment and internal structure changes triggered the applied stress. As time progresses, the process disentanglement advances further, eventually reaching a state where there is an approximate balance between the internal accumulated stresses and externally applied stresses. Consequently, the reduction in stress becomes slower during the later stages of the relaxation process.

Given that pivotal role of internal stress in governing the overall shape memory performance, it is anticipated that the effect of holding time observed in stress relaxation would be reflected in the shape memory effect accordingly. The duration of holding time during stress relaxation is expected to directly impact the resulting shape memory properties of the polymer blend.

PLA Content [%]	0 min Stress [MPa]	1min Stress [MPa]	2min Stress [MPa]	4min Stress [MPa]	6min Stress [MPa]
0	2.76	2.13	1.98	1.84	1.75
20	1.45	1.02	0.91	0.81	0.75
35	1.41	0.91	0.80	0.68	0.60
50	1.17	0.62	0.51	0.40	0.33
100	0.56	0.24	0.15	0.069	0.033

Table 5.2 Data on stresses of polymer blends with varying holding times under tension

5.3.2 Crystallization Behaviours Characterization

After holding the stretched sample at elevated temperature for specific holding time, the

subsequent step involves cooling the sample to stabilize its temporary shape. During this cooling phase, several activities occur, including melt crystallization, which directly impacts the internal structures of these samples programmed with their temporary shapes. DSC analyses were performed to gain better insights into the thermal behaviors of these samples.

The investigation focused on the thermal behavior analysis of TPU/PLA polymer blend samples at their temporary shapes. Heat-cool-heat cycles were conducted in all DSC analyses. The first heat cycle reveals the immediate state of samples that have experienced various holding times, providing direct insights into their thermal behaviours upon memorizing their temporary shapes. Meanwhile, the second heat cycle illustrates the thermal behaviors of samples upon the removal of the thermal history during the sample preparation and the shape memory step.

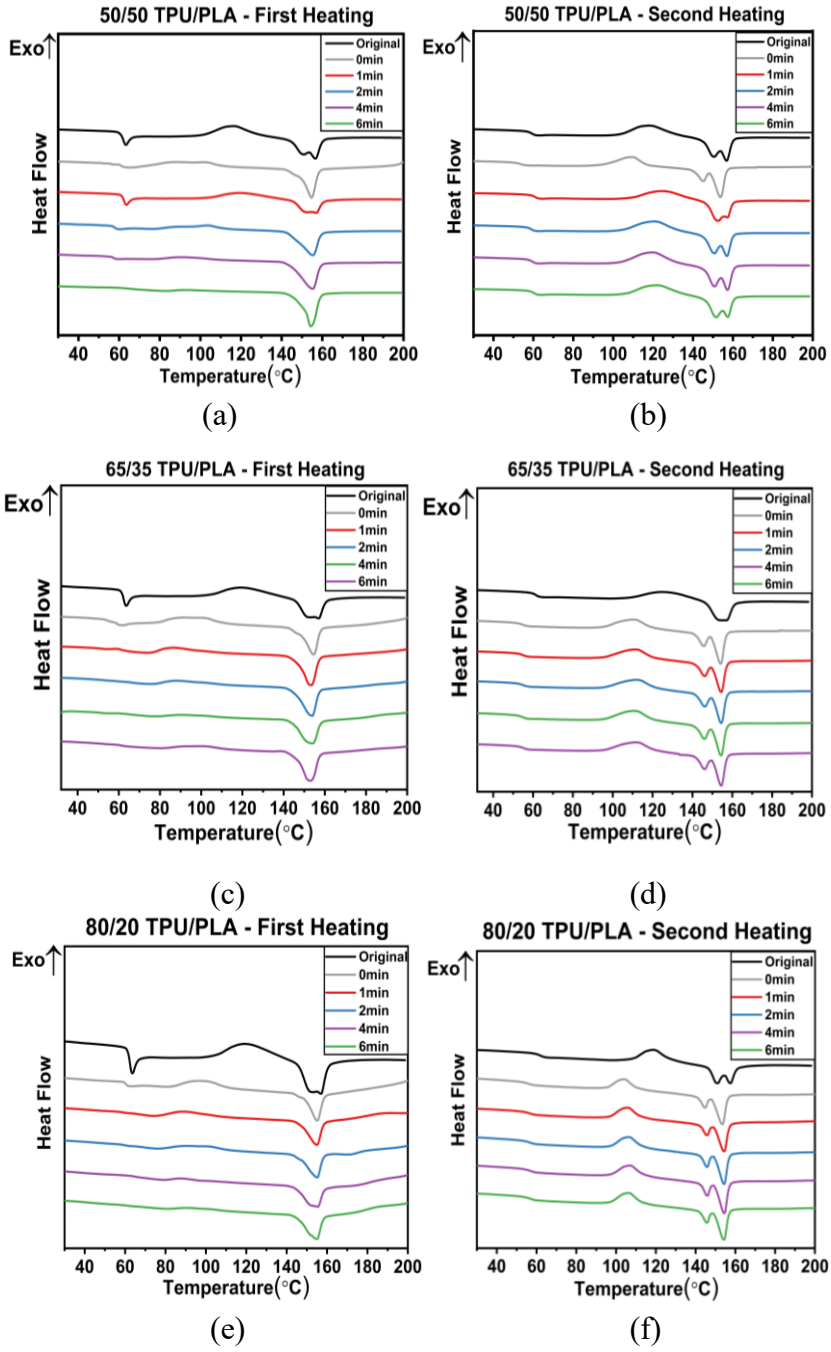

Figure 5.2 DSC curves for TPU/PLA polymer blends with various holding times (none, 1 min, 2min, 4min, 6min): (a)(b) 50/50 TPU/PLA (c)(d) 65/35 TPU/PLA (e)(f) 80/20 TPU/PLA

Figure 5.2 illustrates the first and second heat cycles of the fabricated and programmed samples that underwent different holding times in the DSC tests. Figures 5.2 (a), (c), and (e) highlight significant differences among the samples. Extended holding periods result in a reduction of the cold crystallization peak at approximately 120˚C. Particularly in the sample held for 6 minutes, the cold crystallization peak is notably inconspicuous on the DSC thermogram. Conversely, the melting peak at approximately 150 ˚C becomes more prominent and sharper with increasing holding time. Combined with the key data obtained from analyses of DSC thermograms in Table 5.3, it can be seen that for the 50/50 TPU/PLA polymer blend, the enthalpy of cold crystallization decreases from 14.92 J/g to 1.13 J/g, while the melt crystallization enthalpy increases from 18.58 J/g to 21.16 J/g as the holding time increases from 0 to 6 minutes. Similar trends are observed across samples with other compositions. Additionally, polymer blends with higher PLA contents, prepared using the same holding time, consistently show higher degree of crystallinity.

These observed phenomena are closely linked to crystallization behaviors, particularly pertaining to melt crystallization during the cooling process in Step 4 of the shape memory test cycle and subsequent cold crystallization upon the first heat cycle in the DSC test. The sustained tensile strain during the holding period of the shape memory test cycle facilitates strain-induced crystallization.[103] Therefore, a longer holding time under tension enhances polymer chain

alignment along the straining direction, leading to a more structured arrangement and reduced entanglements within samples. This, in turn, promotes crystal growth, ultimately resulting in higher degree of crystallinity and improved crystalline completeness for samples. As most crystals form during melt crystallization in the programming steps of the shape memory polymer blend, the subsequent cold crystallization, functioning as a complementary crystallization process, becomes constrained. Consequently, due to limited cold crystallization, samples possess predominantly only one crystalline form. This is evident by the sharper melting peaks, which consolidate into a single distinct peak in the DSC thermograms.

Time [min]	ΔHcc[a)] [J/g]	ΔHm[b)] [J/g]	Xc[c)] [%]	Xt[d)] [%]
None	14.92	18.58	7.81	3.91
0	13.36	18.68	11.36	5.68
1	6.83	18.89	25.74	12.87
2	6.45	20.57	30.14	15.07
4	4.04	21.71	37.72	18.86
6	1.13	21.16	42.76	21.38

(a)

Table 5.3 DSC data for TPU/PLA polymer blends with various holding times: none (original sample), 0min, 1 min, 2min, 4min, 6min: (a) 50/50 TPU/PLA (b) 65/35 TPU/PLA (c) 80/20 TPU/PLA

Time [min]	ΔHcc[a)] [J/g]	ΔHm[b)] [J/g]	Xc[c)] [%]	Xt[d)] [%]
None	9.86	11.37	4.60	1.61
0	8.51	11.84	10.15	3.55
1	5.05	12.49	22.69	7.94
2	3.81	13.09	28.30	9.91
4	2.38	13.19	32.96	11.54
6	2.73	14.30	35.28	12.35

(b)

Time [min]	ΔHcc[a)] [J/g]	ΔHm[b)] [J/g]	Xc[c)] [%]	Xt[d)] [%]
None	5.46	6.18	3.84	0.77
0	4.40	6.55	11.47	2.30
1	3.25	6.79	18.89	3.78
2	2.98	6.92	21.02	4.20
4	0.95	6.97	32.12	6.42
6	1.07	7.22	32.82	6.56

(c)

a) Cold crystallization enthalpy; b) Melting enthalpy; c) Crystallinity of PLA; d) Crystallinity of the entire polymer blend

Table 5.3 DSC data for TPU/PLA polymer blends with various holding times: none (original sample), 0min, 1 min, 2min, 4min, 6min: (a) 50/50 TPU/PLA (b) 65/35 TPU/PLA (c) 80/20 TPU/PLA [continue]

However, these features seem to diminish in the second heat curve as depicted in Figure 5.2 (b), (d) and (f). The DSC thermograms of all samples exhibit similar profiles during the second

heat cycles, which implies nearly consistent cold crystallization peaks and double melting peaks. Considering the 50/50 TPU/PLA polymer blend as a representative example, as shown in Figure 5.3, the degree of crystallinity contributed by the initial melt crystallization evaluated in the first heat cycle significantly increases with longer stretching durations; however, the melt crystallinity curve of the second heating is rather flat. This indicates that upon heating above the melting point of PLA during the first heat cycle, all PLA crystals melt and the entire thermal history of the polymer blend samples have been removed. All samples acquire a comparable inner structure after the completion of the first heat and cool cycles under the same cooling condition and will exhibit similar crystallinity upon reheating in the absence of external tensile forces.

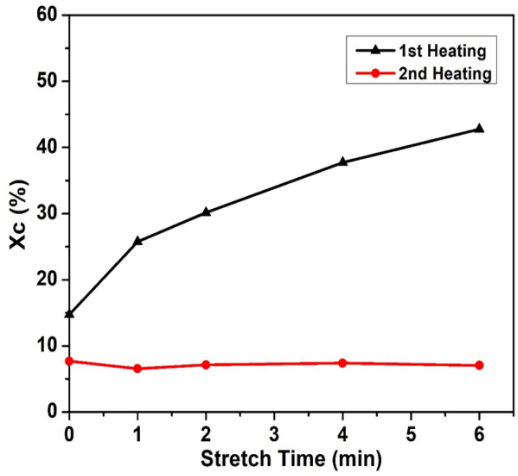

Figure 5.3 Degree of melt crystallinity of 50/50 TPU/PLA polymer blends in DSC tests on first and second heat cycles

5.3.3 Shape Memory Effect Characterization

To precisely evaluate the effect of holding time during the sample programming sequence on shape memory performance, SME characterization measurements were performed on samples with specified compositions and hold durations. Furthermore, the relationship between holding time and shape memory performance is meticulously elucidated, providing details insights from various perspectives.

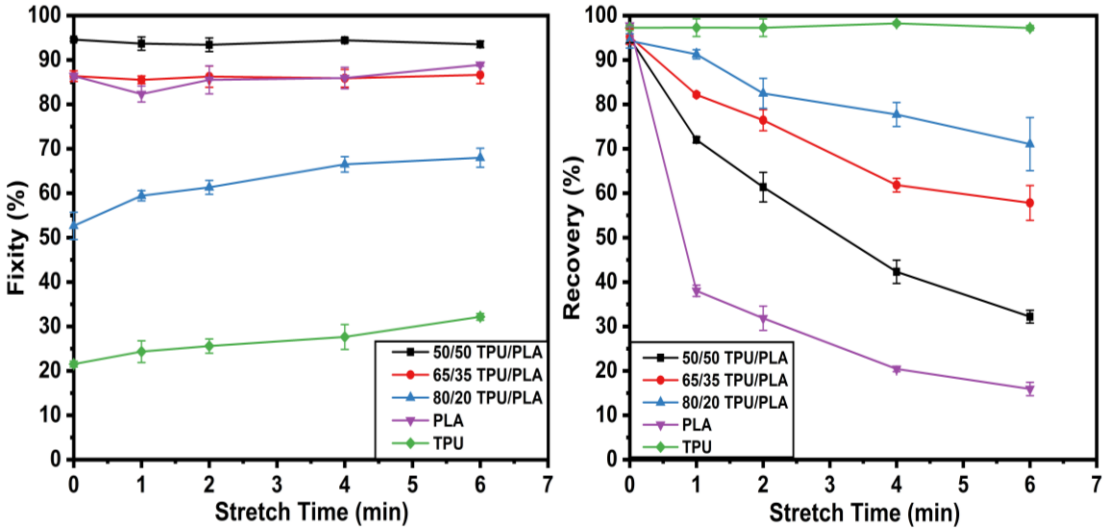

(a) (b)

Figure 5.4 Shape memory effect characterization of TPU/PLA polymer blends with various stretching lengths: (a) fixity (b) recovery

The fixity and recovery rates for samples subjected to different holding times are depicted in Figures 5.4 (a) and (b), respectively. In Figure 5.4 (a), it can be seen that the differences in fixity

due to composition exhibit more pronounced variations, while differences attributed to the holding period are comparatively lower. Reviewing the data summarized in Table 5.4 (a), it is evident that the fixity marginally increases by approximately 5% to 10% with increasing holding time. Interestingly, for certain compositions such as the 50/50 TPU/PLA polymer blend, the fixity remains virtually constant, with a mere 1% difference when holding time increases. Only TPU and 80/20 TPU/PLA polymer blend show p-values less than 0.05, indicating that different stretching times cause significant differences in their fixity for these compositions.

Conversely, Figure 5.4 (b) demonstrates significant variation in recovery across most samples as the holding time changes. For instance, the pure PLA sample exhibits a dramatic drop in recovery by nearly 60%when the stretching hold time varies from 0 min to just 1 min. Similarly, in the case of the 50/50 TPU/PLA polymer blend, the recovery drops from 94.20% to 32.21% when the holding time increases from 0 min to 6 min. Except for the pure TPU, all the other samples also realize a significant decrease in the recovery rate.

PLA Content [%] / Holding time [min]	0	20	35	50	100
0	21.52 ± 0.66	52.65 ± 3.07	86.37 ± 1.20	94.59 ± 0.33	86.39 ± 0.64
1	25.19 ± 2.45	59.44 ± 1.14	85.54 ± 0.87	93.70 ± 1.50	82.33 ± 1.82
2	25.59 ± 1.59	61.32 ± 1.55	86.25 ± 2.39	93.43 ± 1.54	85.53 ± 3.16
4	29.62 ± 2.80	66.50 ± 1.74	85.88 ± 1.99	94.44 ± 0.51	85.94 ± 2.40
6	32.17 ± 0.74	67.99 ± 2.14	86.65 ± 1.96	93.53 ± 0.74	88.92 ± 0.31

(a)

PLA Content [%] / Holding time [min]	0	20	35	50	100
0	97.27 ± 0.57	94.32 ± 1.61	95.27 ± 1.74	94.92 ± 1.02	97.76 ± 0.12
1	97.30 ± 1.99	91.30 ± 1.01	82.20 ± 0.45	72.03 ± 0.66	38.03 ± 1.26
2	97.28 ± 1.98	82.49 ± 3.39	76.45 ± 2.38	61.38 ± 3.38	31.85 ± 2.74
4	98.26 ± 0.37	77.74 ± 2.70	61.84 ± 1.54	42.31 ± 2.63	20.43 ± 0.60
6	97.23 ± 0.53	71.01 ± 5.98	57.82 ± 3.92	32.21 ± 1.46	15.93 ± 1.51

(b)

Table 5.4 shape memory effect characterization values of TPU/PLA polymer blends with various stretching lengths: (a) fixity (b) recovery

The discussion here focuses on how the holding time influences the residual stress and the

degree of crystallinity within the samples. First, it's necessary to discern between the original crystals within the programmed polymer blend and the newly formed crystals induced by the stretching process. As it is known that the crystals present in the molded sample prior to the shape memory test sequence would not melt throughout the process, these crystals act as pivotal nodes, storing energy and aiding in the recovery to the original shape. [60,61] Unlike the original crystals, the newly formed crystals emerged during the stretching process are distributed throughout the deformed temporary shape along a number of newly ordered polymer chains. They construct a physical network over the temporary shape and can be assumed to play a significant role in maintaining the temporary shape (i.e., fixity) rather than in reinstating the original shape (i.e., recovery).

Two competing factors occur within the polymer blends. On the one hand, the presence of newly formed crystals should contribute to the fixation of the samples' temporary shapes because of the physical hinderance. On the other hand, the amorphous region diminishes as the degree of crystallinity increases, counteracting the fixation process. Consequently, the increase in holding time does not cause a significant change in fixity, except for a few polymer blends with higher TPU content, where a marginal increase in fixity is observed.

Regarding recovery, the residual stress within the sample plays a dominant role and acts as a driving force supporting the recovery process. However, observations from previous

characterization indicate that increased holding time correlates with decreased internal stress. When coupled with the newly formed crystals that can support the temporary shape, this leads to an inevitable decrease in recovery.

Figure 5.5 illustrates the shape memory characterization results in relation to the PLA content in the polymer blends. The variability of fixity due to stretching time appears quite consistent across different compositions, while the p-values are smaller than 0.05 for all compositions with PLA content as the variable. This reveals that the effect of stretching time on fixity is limited, with fixation depending more on the blend composition within the sample. In contrast, higher PLA content influences recovery more significantly than the holding time during stretching. In polymer blends with elevated PLA content, the change in both degree of crystallinity and internal stress are more pronounced within the blend, resulting in reduced resistance to changes in holding time.

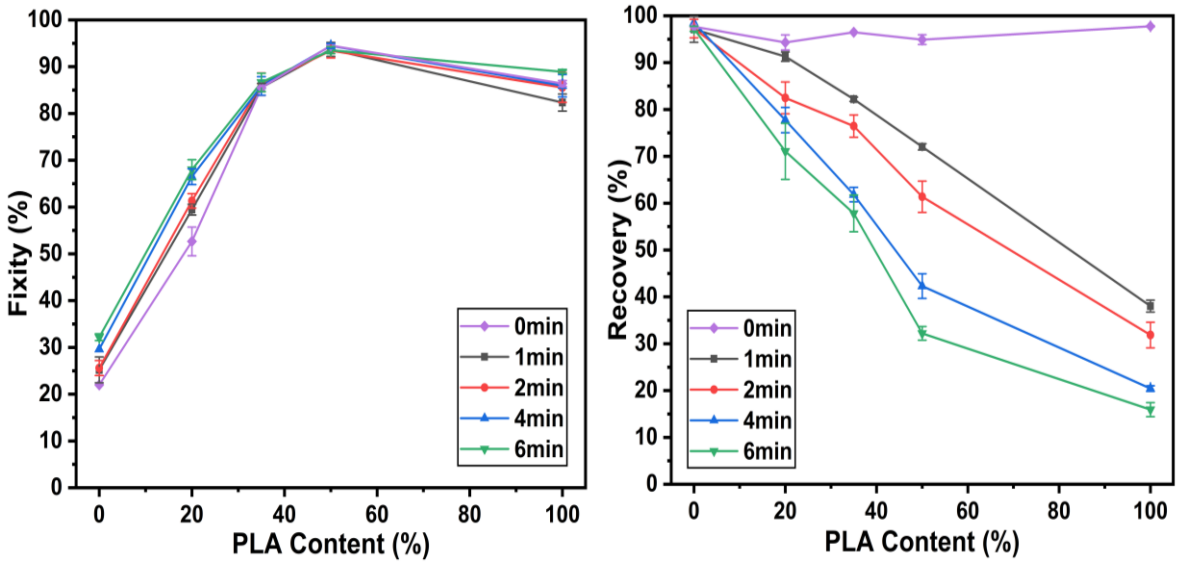

(a) (b)

Figure 5.5 Shape memory effect characterization of TPU/PLA polymer blends as a function of the PLA content: (a) fixity (b) recovery

Given the substantial influence of residual stress on shape memory performance, particularly on recovery, understanding the relationship between the internal stress and the associated shape memory properties becomes crucial. To delve deeper into this correlation, the internal stress retention and recovery ratios are plotted on the same graph. This visualization aims to offer a clearer comparison of the decline patterns and trends, facilitating a better understanding of how these factors evolve in tandem.

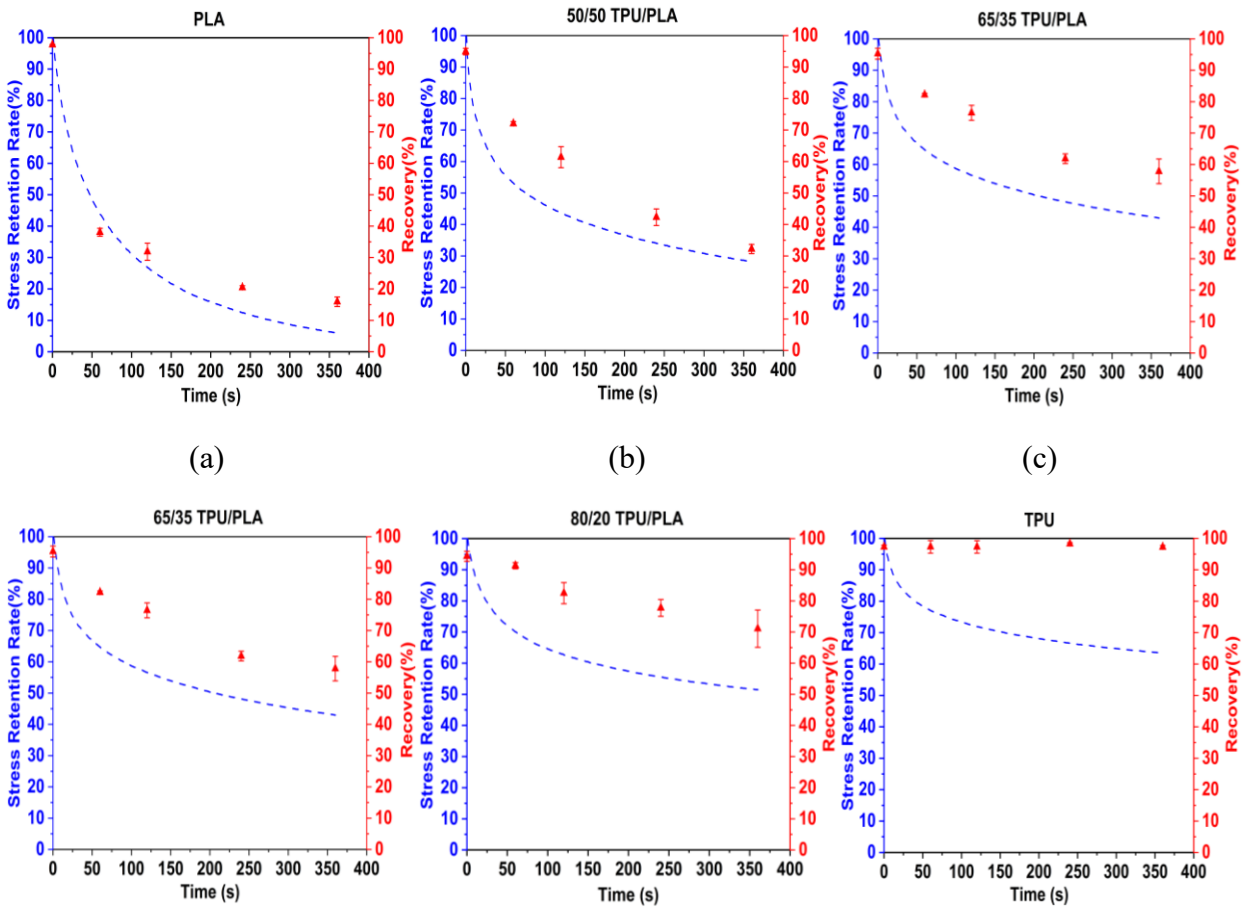

Figure 5.6 Decreasing trend of the residual stress and recovery at increasing holding duration: (a) PLA (b) 50/50 TPU/PLA (c) 65/35 TPU/PLA (d) 80/20 TPU/PLA (e) TPU

Figure 5.6 illustrates the simultaneous decreases in residual stress and recovery with increasing holding times. As PLA content increases, the recovery data points appear align more closely with the stress curve. In the case of the pure PLA sample, the recovery data points are virtually consistent with the stress curve. Conversely, for the pure TPU samples, the recovery

points follow a relatively flat pattern, displaying minimal correlation with the stress curve. This observation suggests that higher TPU content reduces the dependence of recovery on the change in holding time. Considering the stress measurements provided earlier, it could be hypothesized that elevated stress levels might mitigate the effects induced by the holding time, contributing to greater consistency in the recovery.

5.4 Conclusion

The focus of this chapter revolves around the impact of the holding time during stretching at the transition temperature, specifically emphasized as step 3 within the shape memory testing sequence depicted in Figure 3.8. It delves into the examination and analysis of how this factor influences the shape memory properties of TPU/PLA polymer blends.

The designated holding durations for investigation range from 0 to 6 minutes. Various blend compositions, including 50/50, 65/35 and 80/20 TPU/PLA polymer blends, alongside pure PLA and pure TPU were systematically characterized. Experimental results revealed that a direct correlation between increased holding time and reduced residual stress within the samples due to the stress relaxation effect. Simultaneously, the stretching process induced a higher degree of crystallinity, thereby affecting the shape memory properties directly. Fixity showed slight improvement with longer holding time, while the recovery substantially decreased, particularly in

samples with low TPU content. Moreover, the relationship between the shape memory properties and the stored stress within the physical network of the samples was explored. The recovery behaviour in samples with higher PLA contents demonstrated a stronger correlation with the trend of the internal stress, significantly improving increased TPU content.

In essence, the duration of holding time in the typical shape memory cycle emerged to be a critical factor influencing the shape memory properties of TPU/PLA polymer blends. The PLA's crystalline region was observed to comprise original crystals formed during the sample fabrication and the newly generated crystal formed during the shape memory test sequence. Each of these two crystalline structures impacting the material's shape memory performance differently. These findings pose constraints on both processing and utilization of the material. Therefore, avenues to improve the shape memory properties of TPU/PLA polymer blends and to reduce the reliance of on the holding time warrant further exploration and study.

Chapter 6. Influence of Cooling Methods on Shape Memory Effect

6.1 Introduction

The crystallization of individual components in polymer blends significantly influences their mechanical properties and shape memory performance. Therefore, special attention is given to the cooling process, a crucial step leading to crystallization, during sample preparation. The cooling conditions, encompassing temperature range of cooling and cooling rate, are pivotal factors. As the molding temperature has been pre-determined, this chapter focuses on the effect of cooling methods on the crystallization behaviors of TPU/PLA blend, and thereby the resulting shape memory performance.

Characterization studies were performed on TPU/PLA polymer blends fabricated by slow cooling, air cooling, and water cooling, resulting in rough estimates of cooling rates ranging from 0.01 ˚C/s to 0.05 ˚C/s to 1 ˚C/s. The experimental results demonstrated that a slower cooling rate led to higher degree of crystallinity within the polymer blends. Consequently, this elevated the residual stress, impacting the shape memory properties. It was noted that a higher degree of crystallinity correlated with increased shape recovery but reduced fixity. This observation indicates

the heightened crystallinity primarily contributes to greater stored stress for shape recovery within the TPU/PLA system. Moreover, the increase in crystallinity led to a decrease in the amorphous region of PLA, thereby impeding the fixity of the temporary shape. By adjusting the cooling rate, an endeavour was made to address the significant recovery decline with prolonged holding time reported in the previous chapter.

6.2 Experimental

This chapter investigates the effect of cooling rates on the crystallization and the shape memory properties of TPU/PLA polymer blends. Three cooling methods, namely water cooling, air cooling, and slow cooling, were chosen to represent the different cooling rate levels (i.e., rapid, moderate, and slow, respectively).

Water cooling signifies a method characterized by a rapid cooling rate of approximately 1 ˚C/s. It involves the use of a setup comprising two cooling plates through which cool water circulates, as depicted in Figure 3.2 from Chapter 3. The flow of water aids in accelerating the cooling process. Air cooling denotes a moderate cooling rate of approximately 0.05 ˚C/s, where samples are cooled by natural convection in air at room temperature. Lastly, slow cooling involves a deliberately slower cooling rate of about 0.01 ˚C/s. In this case, samples are retained within the hot compression molding machine with the heaters turned off, allowing them to be cooled

gradually along with the machine.

In order to facilitate a more comprehensive comparison and understanding of the effects associated with different conditions, the samples being discussed in this chapter consist of 50/50 TPU/PLA, 65/35 TPU/PLA, and 80/20 TPU/PLA polymer blends. Each composition was studied across various holding times and cooling methods. The experimental designs corresponding to this chapter are detailed in Table 6.1. To ensure the repeatability of data, at least three samples of the same species were tested for each characterization method. Refer to Chapter 3 for more details on the experimental procedures.

Sample Designation	TPU (wt%)	Holding times (min)	Cooling Methods
50/50 TPU/PLA	50	0, 1, 2, 4, 6	Water, Air, Slow
65/35 TPU/PLA	65	0, 1, 2, 4, 6	Water, Air, Slow
80/20 TPU/PLA	80	0, 1, 2, 4, 6	Water, Air, Slow

Table 6.1 Summary of sample ratios, holding times, and cooling methods

6.3 Results and Discussion

6.3.1 Effect of Crystallization

The cooling rate is considered to be a critical factor affecting the sample crystallization. Therefore, the initial focus of this chapter is on the characterization of the crystallization behaviors,

providing a foundation for subsequent discussion of various analyses in this part of the studies.

Figure 6.1 illustrates the DSC thermograms for samples across all compositions and cooling methods. From the graph, it is apparent that higher cooling rates correspond to larger cold crystallization peaks. In Figure 6.2 (a), the slow colling curve exhibits an indiscernible cold crystallization peak. Additionally, data summarized in Table 6.2 suggests that higher cooling rates tend to result in lower degree of melt crystallinity. Moreover, there is a slight increase in the glass transition temperature with increasing cooling rate. Although DSC thermographs of air-cooled and water-cooled 50/50 and 65/35 TPU/PLA polymer blends manifest distinct differences in cold crystallization and melting peaks, the calculated values of the degree of melt crystallinity are remarkably similar.

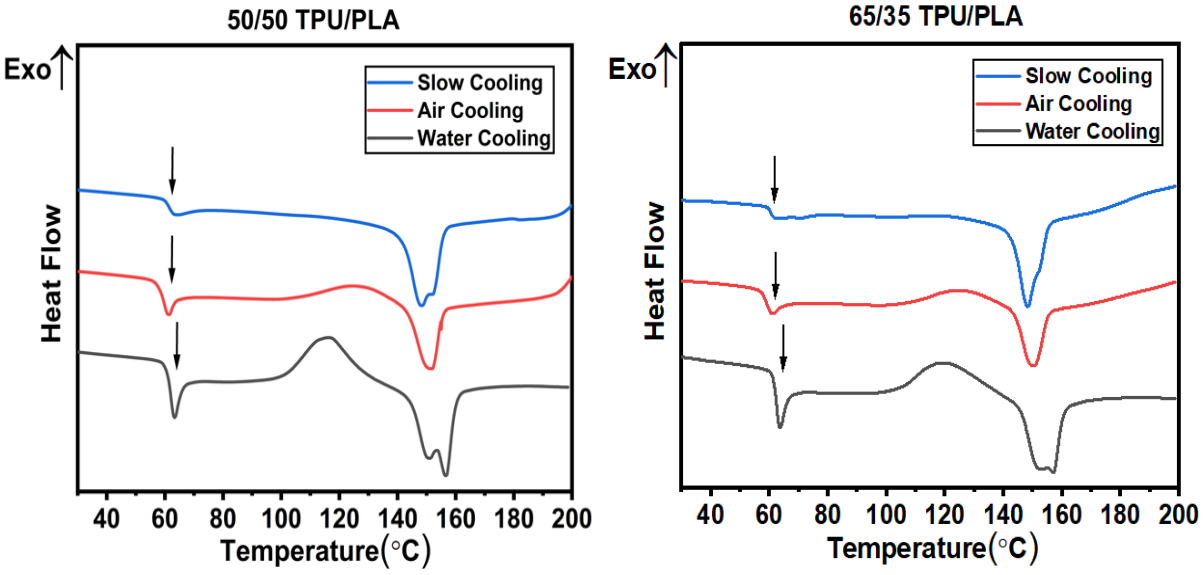

(a)

(b)

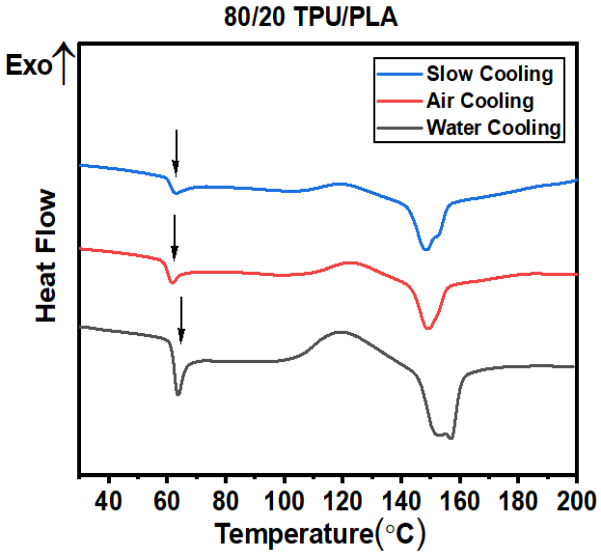

(c)

Figure 6.1 DSC curves of polymer blends prepared by various cooling methods: (a) 50/50 TPU/PLA (b) 65/35 TPU/PLA (c) 80/20 TPU/PLA sample

The crystallization process is commonly understood to occur through two primary stages:

nucleation and growth. PLA nucleation is a relatively slow process, requiring an extended period to reach completion.[90] Furthermore, crystal growth occurs before polymer chains become immobilized, occurring prior to the amorphous region reaching the glassy state.[104] Hence, slower cooling rates, especially exemplified by the slow cooling method in this research, facilitate higher melt crystallinity by allowing sufficient time for crystal nucleation and growth.[90,105,106] On the other hand, the cold crystallization detected in the DSC thermogram initiates from nuclei formed during the preceding cooling process but does not have sufficient time to grow. [92] Consequently, faster cooling rates, such as those exhibited by water cooling or air cooling, result in more pronounced cold crystallization.

Interestingly, the air-cooled and water-cooled samples demonstrate minimal differences in terms of their degrees of melt crystallinity. Drawing reference to the crystallization behaviour of other semi-crystalline polymers like polypropylene, it can be inferred that this phenomenon may arise due to the fact that only lower cooling rates exert a significant effect on crystallinity. [91] Conversely, when the cooling rate goes above a critical value, its impact on melt crystallinity suppresses considerably. Further investigation can verify this assumption by controlling the cooling rate in a more precise manner.

PLA content [%]	Cooling Method	ΔHcc[a)] [J/g]	ΔHm[b)] [J/g]	Xc[c)] [%]	Xt[d)] [%]
20	Slow	3.39	6.65	17.40	3.48
	Air	4.18	5.67	7.95	1.59
	Water	5.46	6.18	3.84	0.77
35	Slow	2.43	9.28	20.89	7.31
	Air	4.51	6.11	4.88	1.71
	Water	9.86	11.37	4.60	1.61
50	Slow	/	15.67	33.45	16.73
	Air	6.30	10.10	8.11	4.06
	Water	14.92	18.58	7.81	3.91

a) Cold crystallization enthalpy; b) Melting enthalpy; c) Crystallinity; d) Crystallinity of the entire polymer blend

Table 6.2 DSC data of polymer blends prepared by various cooling methods: (a) 50/50 TPU/PLA (b) 65/35 TPU/PLA (c) 80/20 TPU/PLA sample

6.3.2 Stress Relaxation Tests

The primary focus of this chapter centers on evaluating the cooling rate through various cooling methods. Figure 6.2 shows the stress relaxation effects observed in samples subjected to different cooling methods. It is noted that Figure 6.2 (a) displays the results of only the air-cooled and water-cooled 50/50 TPU/PLA blends samples instead of all three methods. This is due to the fact that the 50/50 TPU/PLA sample becomes excessively rigid under the slow cooling method.

Consequently, these samples experience fracture at approximately 15% strain during stretching before stress relaxation in the shape memory test sequence, rendering further relevant characterizations infeasible.

Across all graphs, the curves for air-cooled and water-cooled samples exhibit remarkable similarity. In particular, the curves of the 50/50 TPU/PLA and 80/20 TPU/PLA samples almost entirely overlap, demonstrating negligible differences. In Figures 6.2 (b) and (c), the stress curves for slow cooling notably display higher stresses compared to the other methods. For the 65/35 TPU/PLA sample, the curve of the slow-cooled sample consistently maintains higher stress levels than other samples throughout the test. In contrast, the curve of the slow-cooled sample with 80/20 TPU/PLA ratio starts with stress level similar to the samples made by other cooling methods but subsequently exhibits higher stresses at later stages.

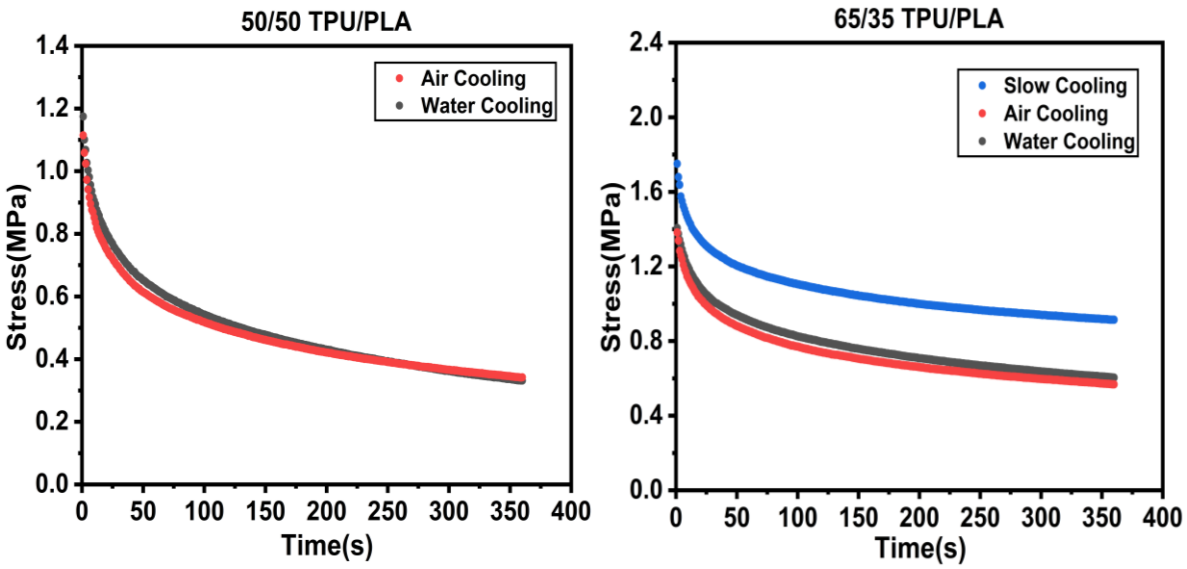

(a) (b)

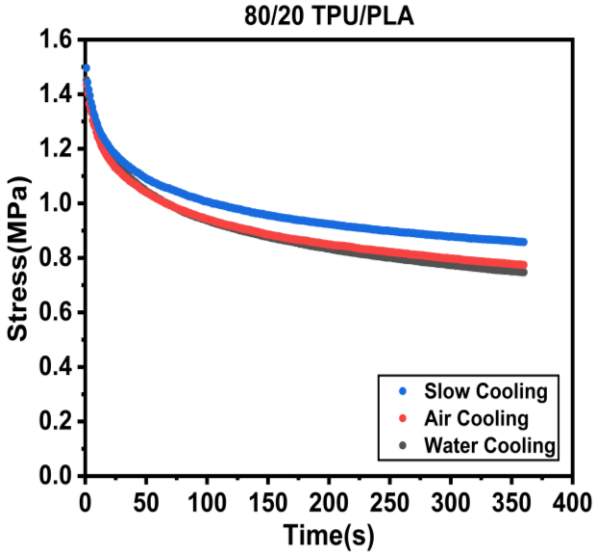

(c)

Figure 6.2 Stress Relaxation of polymer blends produced by varying cooling methods

These observed phenomena can be effectively analyzed in conjunction with the crystallization behaviours detailed in the preceding section. The microstructural aspects,

encompassing physical network density and crystallization behaviors, exhibit similarities among samples prepared by the air cooling and water cooling methods. Consequently, the stress patterns corresponding to these two methods are notably alike. Conversely, the slow cooling method is found to induce a significantly higher degree of crystallinity in the samples. As a result, greater stresses become necessary to achieve the stretching of samples to the specified 100% strain. In comparison to the 80/20 TPU/PLA sample, the 65/35 TPU/PLA polymer blend comprises a higher proportion of PLA, thereby accentuating the impact of the slow cooling method on its crystallization behaviour and subsequent stress relaxation performance. All these observations collectively serve as evidence to elucidate the performance of subsequent shape memory effect tests, providing valuable insights into the material's behaviour and performance.

Cooling Method	PLA Content [%]	0 min Stress [MPa]	6min Stress [MPa]
Water cooling	20	1.45	0.75
	35	1.41	0.60
	50	1.17	0.33
Air Cooling	20	1.44	0.77
	35	1.38	0.57
	50	1.11	0.34
Slow Cooling	20	1.50	0.86
	35	1.75	0.91
	50	/	/

Table 6.3 Data on stress relaxation of polymer blends produced by varying cooling methods

6.3.3 Shape Memory Effect Characterization

Following the preliminary discussion on internal stresses and crystallization behaviours, the subsequent focus lies on exploring the impact of cooling rate on shape memory properties. This chapter reports comprehensive shape memory effect experiments, integrating all the aforementioned conditions – composition, holding time in the shape memory test sequence, and cooling method.

Figures 6.3(a)-(f) present the fixity and recovery values observed in samples subjected to different holding times and cooling methods, with corresponding data detailed in Table 6.4. As

previously mentioned, the 50/50 TPU/PLA samples produced by the slow cooling method were excessively stiff, impeding completion of the required stretching process. Conversely, the fixity and recovery values for the other two methods display close similarity, with differences predominantly within the 5% range. Similarly, in the case of the 65/35 TPU/PLA polymer blends, the shape memory performance between samples prepared by air cooling and water cooling remains controlled within a 5% range. However, a significant deviation occurs with samples subjected to slow cooling. Contrary to the other methods, slow cooling results in a reduction in fixity by approximately 15-20%, accompanied by a corresponding increase in recovery. Regarding the 80/20 TPU/PLA polymer blends, the cooling method appears to have a limited influence on fixity. It is noted that slow cooling clearly enhances recovery, showcasing a change in recovery rate of around 5% over a 6 minute holding time, unlike the other cooling methods.

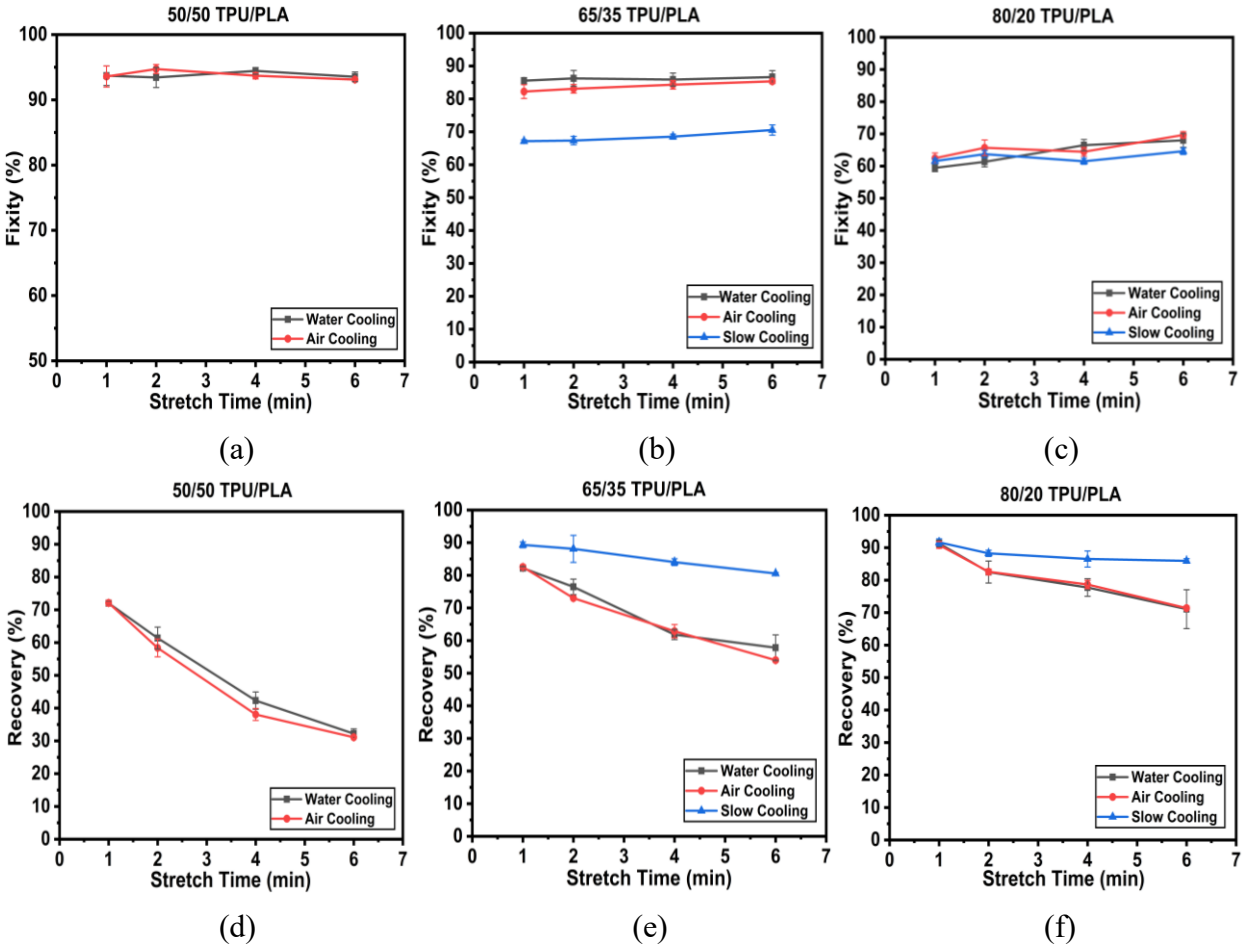

Figure 6.3 Shape memory effect characterization of TPU/PLA polymer blends with varying holding times and cooling methods: (a)(b)(c) fixity (d)(e)(f) recovery

The cooling method after the compression molding of the samples being studied in this chapter occurs during sample preparation, affecting the crystallinity of the original crystals present before characterizing the polymer blend. Given the similarities in internal residual stresses and crystallization behaviours between samples prepared by air cooling and water cooling, minor differences in their shape memory properties were anticipated. Lower cooling rates, such as those

employed in the slow cooling method, substantially increase the degree of crystallinity in the PLA phase. Consequently, the force driving the recovery of the temporary shape back to its permanent shape increases, favoring enhanced recovery. However, the reduced amorphous region of PLA inversely diminishes fixity. In cases involving samples with a higher TPU content, like the 80/20 TPU/PLA polymer blends, the inherent high range of internal stresses reduces the impact of the cooling method on the shape memory effect compared to other compositions. In addition, since slow cooling increases the original degree of crystallinity of the sample, the amount of crystal growth during stretching diminishes. As a result, a slower cooling rate can help minimize the influence of stretching time, contributing to achieving improved consistency in the results. For example, for 80/20 TPU/PLA samples, the use of slow cooling increases the p-value for different stretching times to greater than 0.05, indicating that the effect of stretching time on recovery is not as significant as before.

Holding Time [min]	Slow Cooling		Air Cooling		Water Cooling	
	Rf	Rr	Rf	Rr	Rf	Rr
1	/	/	93.58 ± 1.61	72.10 ± 0.78	93.70 ± 1.50	72.03 ± 0.66
2	/	/	94.72 ± 0.69	58.38 ± 2.71	93.43 ± 1.54	61.38 ± 3.34
4	/	/	93.7 ± 0.49	38.07 ± 1.82	94.44 ± 0.51	42.31 ± 2.63
6	/	/	93.16 ± 0.15	31.10 ± 0.34	93.53 ± 0.74	32.21 ± 1.46

(a)

Holding Time [min]	Slow Cooling		Air Cooling		Water Cooling	
	Rf	Rr	Rf	Rr	Rf	Rr
1	67.15 ± 0.42	89.33 ± 0.87	82.23 ± 2.10	82.55 ± 0.66	85.54 ± 0.87	82.20 ± 0.45
2	67.35 ± 1.27	88.11 ± 4.14	83.09 ± 1.34	73.00 ± 0.49	86.25 ± 2.39	76.45 ± 2.38
4	68.54 ± 0.76	84.04 ± 1.04	84.31 ± 1.32	62.88 ± 2.04	85.88 ± 1.99	61.84 ± 1.54
6	70.54 ± 1.55	80.55 ± 0.30	85.33 ± 0.62	53.99 ± 0.54	86.65 ± 1.96	57.82 ± 3.92

(b)

Holding Time [min]	Slow Cooling		Air Cooling		Water Cooling	
	Rf	Rr	Rf	Rr	Rf	Rr
1	61.55 ± 0.80	91.65 ± 1.07	62.45 ± 1.65	90.83 ± 1.05	59.44 ± 1.14	91.30 ± 1.01
2	63.72 ± 1.14	88.26 ± 0.96	65.71 ± 2.40	82.60 ± 0.84	61.32 ± 1.55	82.49 ± 3.39
4	61.49 ± 0.93	86.52 ± 2.48	64.45 ± 1.38	78.67 ± 1.29	66.50 ± 1.74	77.74 ± 2.70
6	63.91 ± 1.00	85.93 ± 0.69	69.67 ± 1.01	71.39 ± 0.45	67.99 ± 2.14	71.07 ± 5.98

(c)

Table 6.4 Shape memory effect characterization values of polymer blends with varying holding times and cooling methods: (a) 50/50 TPU/PLA (b) 65/35 TPU/PLA (c) 80/20 TPU/PLA

In order to further investigate the correlation between the PLA content within the polymer blend and the influence of the cooling methods on the shape memory properties, a series of graphs are presented in Figure 6.4 as part of this study. Figure 6.4 highlights two distinct stretching times: one minute and six minutes. While the data for the 50/50 TPU/PLA polymer blend prepared by slow cooling is absent from the graph, a discernible pattern emerges, indicating that the slow cooling samples tend to exhibit relatively flatter and less variable trends as the PLA content increases. This trend suggests that a higher degree of crystallinity compensates for the impact of variation in the composition of the polymer blends. Consequently, it implies that slower cooling rates might contribute to better consistency in shape memory performance at different PLA contents as well. This observation implies a potential correlation wherein higher crystallinity resulting from slower cooling rates could potentially aid in maintaining consistent shape memory properties across various PLA content compositions within the blends.

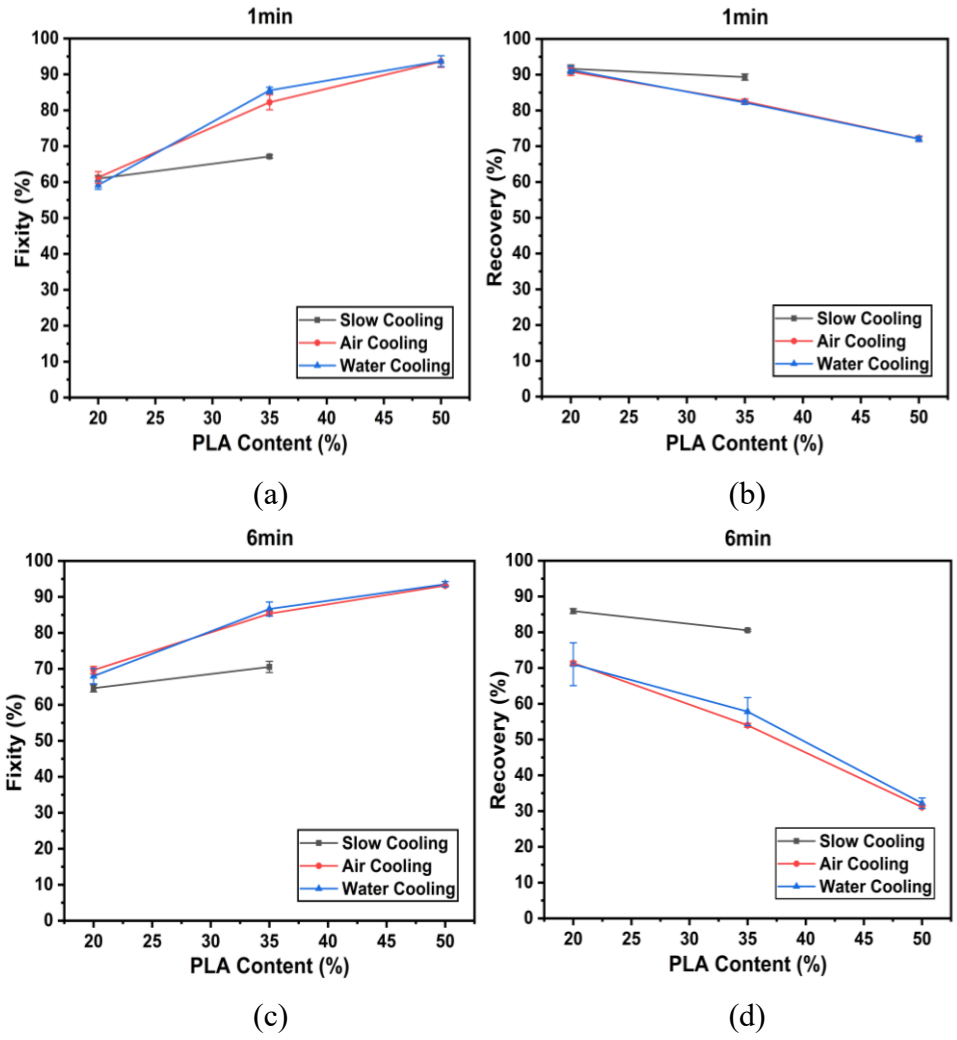

Figure 6.4 Shape memory effect characterization of TPU/PLA polymer blends with varying PLA content and cooling methods: (a) (b) fixity and recovery with 1min stretching time (c) (d) fixity and recovery with 6min stretching time

Building upon the methodology outlined in the preceding chapter, which focused on the characterization of the correlation between the internal stresses and the shape memory properties, the upcoming section will feature a comprehensive comparison and discussion of various cooling

methods.

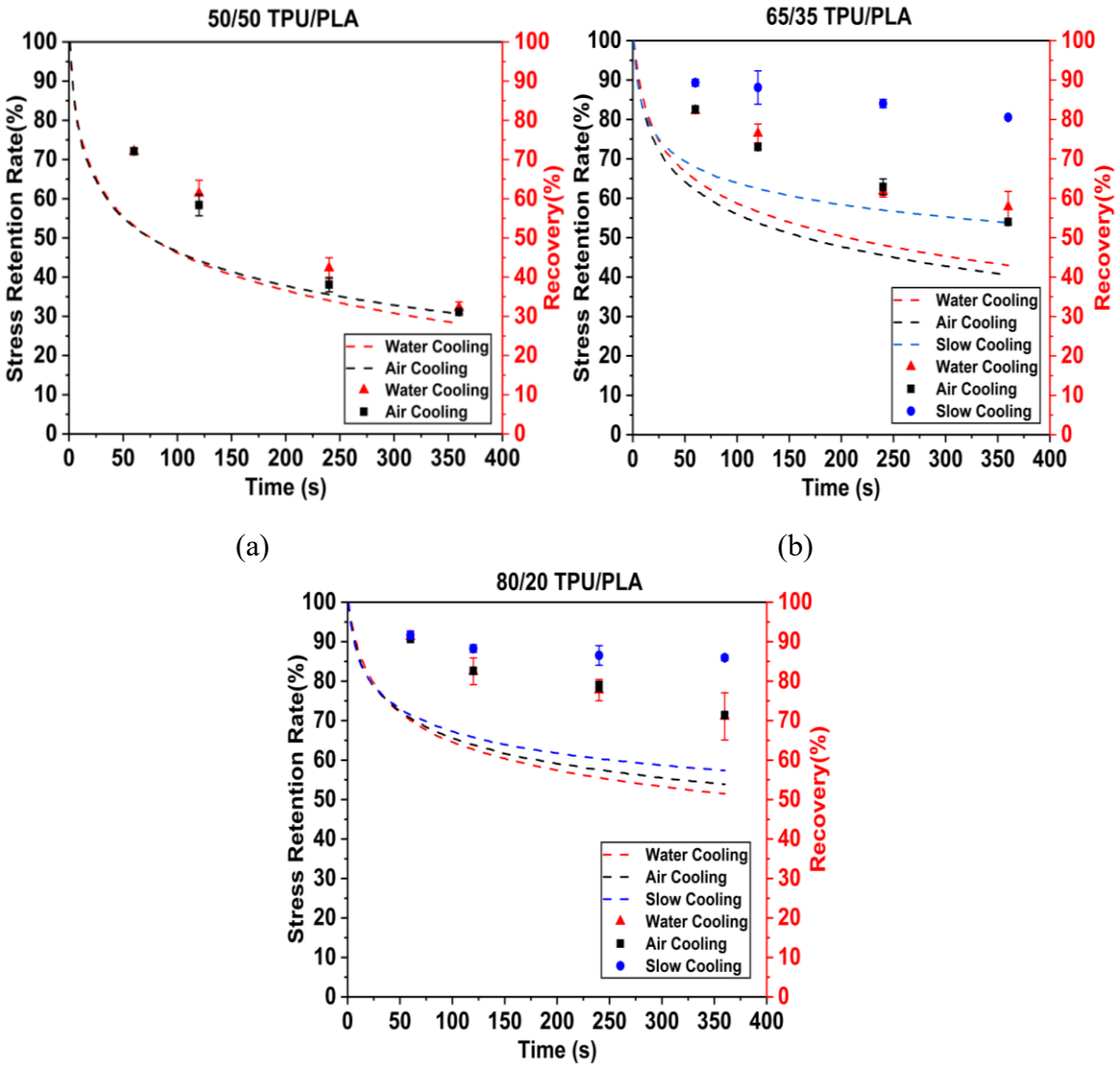

Figure 6.5 Decreasing trend of the residual stress and recovery for polymer blends prepared by varying cooling methods: (a) 50/50 TPU/PLA (b) 65/35 TPU/PLA (c) 80/20 TPU/PLA polymer blends

Figure 6.5 shows the trend depicting the percentage decrease in stress and recovery across different cooling methods. In comparison to samples prepared by water and air cooling, samples subjected to slow cooling exhibit a notably weaker correlation between the recovery rate of and internal stress. For instance, as depicted in Figure 6.5, the recovery of the 80/20 TPU/PLA polymer blend, prepared using slow cooling drops, experiences a slight drop while the stress maintains a sharp decrease similar to the curves for samples prepared by other methods. This observation implies that slower cooling rates might play a role in mitigating the effect of holding time on shape memory performance. Considering the collective data from Figure 6.2 and Table 6.3 in the preceding section, it is evident that a slow cooling rate predominantly amplifies the overall stress level without significantly altering the stress relaxation trend. This indicates a potential scenario where the effect of holding time could be nullified by adequately strong stresses present in the samples.

6.4 Conclusion

This chapter investigates the impact of the cooling methods in sample preparation on the shape memory effect of TPU/PLA polymer blends. In order to reflect varying levels of cooling rates, three cooling methods are selected, which are slow cooling, air cooling and water cooling. And 50/50, 65/35 and 80/20 TPU/PLA polymer blends are prepared through these three cooling

methods, respectively.

Of the various characterizations, slow-cooled samples reveal remarkable differences, whereas the other two cooling methods appear to show relatively similar performance. This means that when the slow-cooled samples are compared to the other two, not only the crystallinity reaches a higher level, but also the value of stress in the stress relaxation process increases. This ultimately leads to a moderately lower fixity and, in contrast, a significantly higher recovery in assessing the shape memory properties. Additionally, the shape memory properties of slow-cooled samples are shown to be less sensitive to the material composition and the holding time, meaning that a stronger consistency is maintained.

This suggests that the use of a fairly low cooling rate for sample preparation is an effective tool for improving the recovery of TPU/PLA polymer blends. However, it should also be taken into account that the fixity may also be correspondingly reduced. Also, a lower cooling rate could also maintain more stable shape memory properties for samples that require longer deformation time during processing. This finding could provide a fresh insight into the modification of such polymer blends.

Chapter 7. Enhanced Shape Memory Properties of TPU/PLA/h-BN Polymer Composites

7.1 Introduction

The preceding chapters have underscored the significant roles of material and processing conditions as well as the resultant crystallinity and internal stress on defining the shape memory properties of TPU/PLA polymer blends. Attempts to further advance the properties of TPU/PLA polymer composites can be made by adding appropriate fillers. According to the information mentioned in Chapter 2, hexagonal boron nitride (h-BN) is capable of forming hydrogen bonds with TPU. To enhance and stabilize the shape memory performance, this chapter explores the addition of hexagonal boron nitride (h-BN) particles as fillers to modify the physical network of the polymers.

This chapter investigates TPU/PLA/BN polymer composites containing varying h-BN concentrations, ranging from 0 to 10%. The findings highlight alternations in the internal microstructure due to the incorporation of h-BN, particularly noticing substantial differences with the inclusion of 10 wt.% h-BN. Interestingly, adding 10 wt.% h-BN resulted in an increased degree of crystallinity and stored stress, akin to the effects of slow cooling as discussed in the previous

chapter. As for the shape memory properties, while the introduction of h-BN improved the fixity of the polymer composites, it hindered their recovery.

This suggests that the effect of h-BN may extend beyond simply promote the degree of crystallinity of PLA; it also influences other microstructures of this polymer composite system. Its presence as fillers throughout the matrix of the polymer blend appears to impact not only the crystallization of PLA but also the physical network of TPU itself. This introduces a novel approach to customizing the properties of TPU/PLA/h-BN polymer blend composites with the aim of achieving the desired shape memory performance in a different direction.

This chapter is sub-divided into two sections. The initial focus of this study is to gain a comprehensive understanding of h-BN's role as a filler in the TPU/PLA polymer composite system. As a result, Part I centers on 50/50 TPU/PLA polymer composites varying contents of h-BN as filler to investigate the effect of h-BN concentration on the shape memory properties. Part II of the study expands its scope to encompass polymer composites with various TPU/PLA ratios. Informed by the outcomes of Part I, specific h-BN contents are chosen in Part II to be added to TPU/PLA polymer composites with differing TPU/PLA ratios to study the effect of h-BN. Experimental

7.2 Experimental

7.2.1 Materials and Design

7.2.1.1 Part I

The materials utilized in this chapter comprise PLA, TPU, and h-BN. More comprehensive information regarding these materials and experimental processes can be referred to in the experimental section of Chapter 3. In Part I, the h-BN content ranged from 0 wt.% to 10 wt.%, as detailed in Table 7.1, and various characterizations relating to shape memory properties were performed on these samples. Alongside the h-BN content, the holding time, as described in Chapter 5, was also taken into account for thorough evaluation and analysis.

Sample Designation	TPU/PLA	Polymer [wt%]	h-BN [wt%]
50/50 TPU/PLA	50/50	100	0
50/50 TPU/PLA-3	50/50	97	3
50/50 TPU/PLA-5	50/50	95	5
50/50 TPU/PLA-10	50/50	90	10

Table 7.1 Composition of 50/50 TPU/PLA/h-BN polymer composites

7.2.1.2 Part II

Part II studied polymer composites with various TPU.PLA ratios: 50/50 TPU/PLA, 65/35

TPU/PLA, and 80/20 TPU/PLA polymer composites Table 7.2 provides an overview of the sample compositions for Part II.

Sample Designation	TPU/PLA	Polymer [wt%]	h-BN [wt%]
50/50 TPU/PLA	50/50	100	0
50/50 TPU/PLA-10	50/50	90	10
65/35 TPU/PLA	65/35	100	0
65/35 TPU/PLA-10	65/35	90	10
80/20 TPU/PLA	80/20	100	0
80/20 TPU/PLA-10	80/20	90	10

Table 7.2 Composition of polymer composites

7.2.2 Characterization Method

In this chapter, the majority of the characterization methods remain consistent with those presented in Chapter 3, except for the thermal behaviours characterization. The introduction of a new component in the polymer composites necessitates an adjustment in the calculating of the degree of melt crystallinity. Since the thermal behaviours of the h-BN will not be specifically addressed in the DSC test coverage, only the contribution of the weight percentage of h-BN in the samples needs consideration. Consequently, determining the melt crystallinity of the TPU/PLA/h-BN polymer composites could be obtained by applying the updated Equation shown below:

$$X_c = \frac{\Delta H_m - \Delta H_{cc}}{\frac{M_1}{M_1 + M_2 + M_3} \times \Delta H_m^o} \quad (7.1)$$

where M_1 is the mass of PLA; M_2 is the mass of TPU; M_3 is the mass of h-BN; ΔH_m is the melting enthalpy of PLA; ΔH_{cc} is the cold crystallization enthalpy (J/g) of PLA; and ΔH^o_m is the enthalpy of 100% crystallized PLA (93.7 J/g).[101]

7.3 Results and Discussion

7.3.1 Characterization of the effect of BN on 50/50 TPU/PLA polymer composites

7.3.1.1 Stress Relaxation Tests

To investigate the effect of h-BN on the material's microstructure, the stress relaxation activities were assessed for 50/50 TPU/PLA polymer composites filled containing different h-BN contents. Following the previous sections, tests were conducted involving a total of 6 min of stretching to encompass the effect of the holding time.

Figure 7.2 illustrates the stress relaxation curves of the samples, depicting a consistent decreasing trend in stresses across all compositions but notable differences in values. With an increase in the h-BN content within the range of 0 wt.% to 10 wt.%, the internal stress stored in the physical network of the polymer composites increases. Table 7.3 reveals relatively small

difference (i.e., within 0.15 MPa) in stresses among 50/50 TPU/PLA composite samples loaded with 0 wt.%, 3 wt.%, and 5 wt.% of h-BN. In contrast, 50/50 TPU/PLA composite loaded with 10 wt.% h-BN exhibits significantly stronger stress compared to the other compositions.

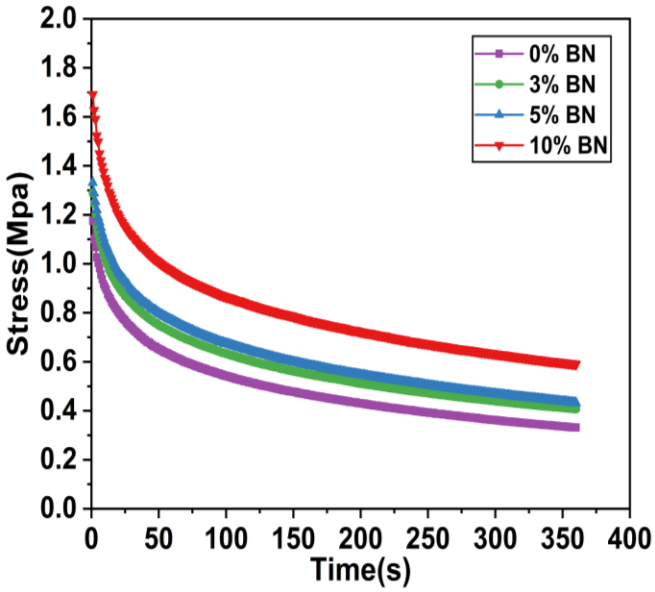

Figure 7.1 Stress Relaxation for 50/50 TPU/PLA polymer composites with diverse BN contents under tension

These results indicate that the addition of h-BN as a filler in polymer composites serves as an effective method for improving the stored stress within the samples. This improvement might stem from the interaction between h-BN and the polymers within the structure. Alternatively, the dispersion of h-BN within the composites' microstructure enhances the obstruction of the polymer chain mobility, consequently augmenting the stress required for tensile stretching. The resulting

increase in internal stress is anticipated to positively affect the shape memory properties of the polymer composites.

BN Content [%]	0min Stress [MPa]	6min Stress [MPa]
0	1.17	0.33
3	1.29	0.41
5	1.33	0.43
10	1.69	0.59

Table 7.3 Initial and final stresses for polymer composites with various BN contents in the process of stress relaxation

7.3.1.2 Crystallization Behaviors Characterization

Building upon the previous section's findings regarding stress relaxation, the utilization of h-BN as a filler has indeed demonstrated its impact on the microstructure of the polymer composites. Given that h-BN possesses good thermal stability, the experiments in this study will not specifically delve into the thermal behaviors of h-BN. such as decomposition. Instead, the focus remains on analyzing the thermal properties of TPU/PLA polymer composites.[82]

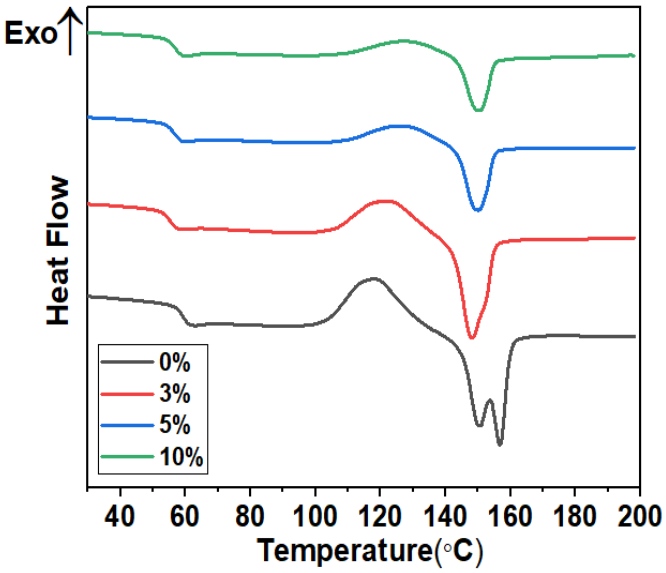

Figure 7.2 DSC curves of 50/50 TPU/PLA polymer composites with diverse BN contents

In order to explore the thermal behaviors of the polymer composites filled with h-BN, DSC analyses were conducted, and the resulting thermograms are presented in Figure 7.3. The neat 50/50 PLA/TPU sample (i.e., without h-BN) exhibits a more pronounced cold crystallization peak and broader double melting peaks. In contrast, polymer composites containing h-BN as filler display sharper and narrower melting peaks as well as smaller cold crystallization peaks. Together with the data summarized in Table 7.4, it can be inferred that higher h-BN content in the polymer composites reduces the enthalpies of cold crystallization and melting, consequently yielding lower degree of net melting crystallinity.

BN Content [%]	ΔHcc[a)] [J/g]	ΔHm[b)] [J/g]	Xc[c)] [%]	Xt[d)] [%]
0	14.92	18.58	7.81	3.91
3	11.71	13.23	3.34	1.67
5	6.39	7.80	3.16	1.58
10	5.69	6.65	2.25	1.13

a) Cold crystallization enthalpy; b) Melting enthalpy; c) Crystallinity. d) Crystallinity of the entire polymer blend

Table 7.4 DSC values of 50/50 TPU/PLA polymer composites with diverse BN contents

The considerable reduction observed in the melting enthalpy signifies that incorporating h-BN as filler in the polymer composites diminishes the overall degree of crystallization. The presence of h-BN is anticipated to trigger heterogeneous nucleation of PLA within the polymer composites. [85,86] However, it also tends to slow down the crystal nucleation rate correspondingly. [107] Consequently, unlike the reported slight facilitation of crystallization of PLA/h-BN composites, which contain only PLA and h-Bn, as reported by Ostrovskiy *et al.*, h-BN exerts an opposing effect on TPU/PLA/h-BN polymer composites. [86] In summary, adding h-BN to TPU/PLA polymer composites appears to be unfavorable to crystallization behaviors.

7.3.1.3 Characterization of Shape Memory Effect

In order to investigate the effect of h-BN on the shape memory properties of the polymer

composites, shape memory effect tests were performed on 50/50 TPU/PLA blend composites with 0%, 3%, 5% and 10% BN as fillers. In addition, the assessment here continues to take into account the holding time in the shape memory cycle as a crucial factor for evaluation.

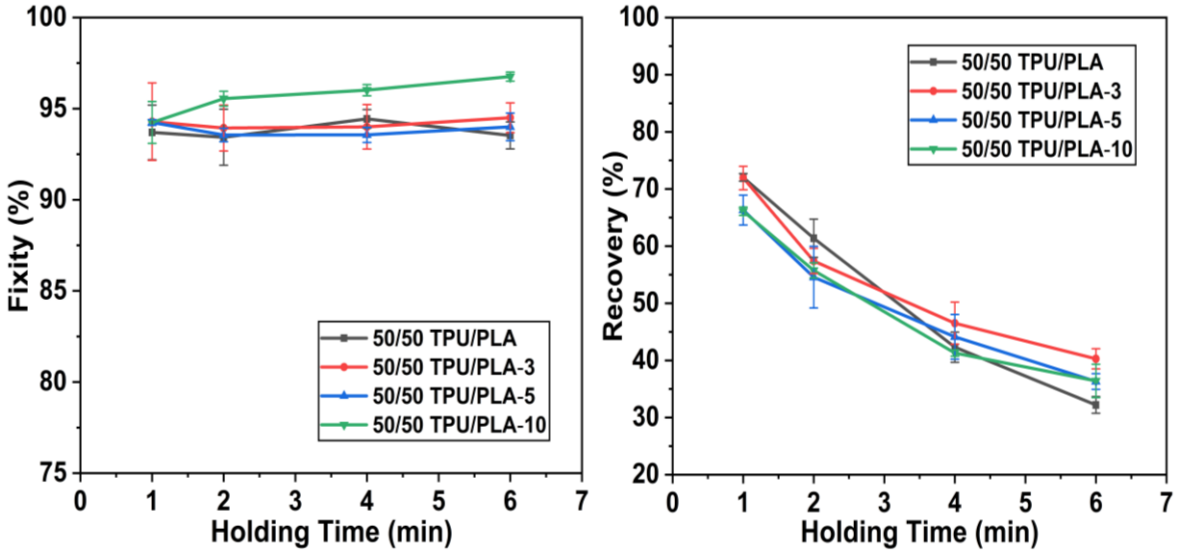

(a) (b)

Figure 7.3 Shape memory effect characterization of 50/50 TPU/PLA polymer composites with varying BN contents and holding times: (a) fixity (b) recovery

Figure 7.4 illustrates the fixity and recovery of the 50/50 TPU/PLA polymer blend composites with h-BN as filler. As indicated in Figure 7.4 (a), the 50/50 TPU/PLA loaded with 10 wt.% h-BN demonstrates more prominent advantages in fixity compared to the samples with lower h-BN contents. However, in Figure 7.4 (b), the curves intersect, making it challenging to discern the specific role of h-BN. Roughly speaking, it is observed that the recovery of the polymer

composite without h-BN exhibits a high level of recovery for samples prepared by a short holding time (e.g. less than 2 minutes). Yet, as the holding times prolongs, especially beyond 2 minutes, the recovery of samples containing h-BN as filler becomes more favorable.

Sample \ Holding time [min]	1	2	4	6
50/50 TPU/PLA	93.7 ± 1.50	93.43 ± 1.54	94.44 ± 0.51	93.53 ± 0.74
50/50 TPU/PLA-3	94.29 ± 2.12	93.94 ± 1.26	94.00 ± 1.22	94.50 ± 0.82
50/50 TPU/PLA-5	94.24 ± 0.16	93.56 ± 0.37	93.56 ± 0.42	94.00 ± 0.76
50/50 TPU/PLA-10	94.25 ± 1.15	95.55 ± 0.41	96.02 ± 0.31	96.76 ± 0.25

(a)

Sample \ Holding time [min]	1	2	4	6
50/50 TPU/PLA	72.03 ± 0.66	61.38 ± 3.34	42.31 ± 2.63	32.21 ± 1.46
50/50 TPU/PLA-3	71.93 ± 2.05	57.40 ± 2.21	46.51 ± 3.68	40.29 ± 1.77
50/50 TPU/PLA-5	66.31 ± 2.62	54.56 ± 5.39	44.13 ± 3.92	36.31 ± 1.37
50/50 TPU/PLA-10	66.12 ± 0.73	55.76 ± 1.32	41.30 ± 0.55	36.41 ± 2.92

(b)

Table 7.5 Shape memory effect characterization values of 50/50 TPU/PLA polymer composites with varying BN contents and holding times: (a) fixity (b) recovery

Among all samples with different h-BN contents tested, only the polymer composite loaded with 10 wt.% h-BN differs significantly from the neat 50/50 TPU/PLA polymer composite. Contrary to the expectation, the 50/50 TPU/PLA loaded with 10 wt.% h-BN exhibits higher fixity, but slightly lower recovery compared to the neat 50/50 TPU/PLA sample. High h-BN content builds a filler network in TPU and contributes to higher internal stress for recovery, but the presence of h-BN particles dispersed in the samples would also disturb the construction of the physical network of the TPU and act as barriers to the movement of the polymer chains simultaneously. [108]. Consequently, the increased stress from the addition of h-BN is inadequate to support a higher recovery. Furthermore, since the addition of h-BN reduces the degree of crystallinity, the proportion of the amorphous phase in PLA becomes more prominent. Therefore, in the 50/50 TPU/PLA polymer blend composite system, the fixity increases remarkably with sufficiently h-BN filler content.

7.3.2 Characterization of the effect of BN on polymer composites with various compositions

7.3.2.1 Stress Relaxation Tests

In the preceding section, it was established that the addition of 10 wt.% h-BN exerts the most noticeable effect on the shape memory properties, with lower filler contents deemed relatively insignificant. Thus, this section focuses solely on investigating polymer composites

filled with 10 wt.% h-BN. Stress relaxation analyses were conducted on 50/50 TPU/PLA, 65/35 TPU/PLA, and 80/20 TPU/PLA blend or their composites filled with and 10 wt.% h-BN.

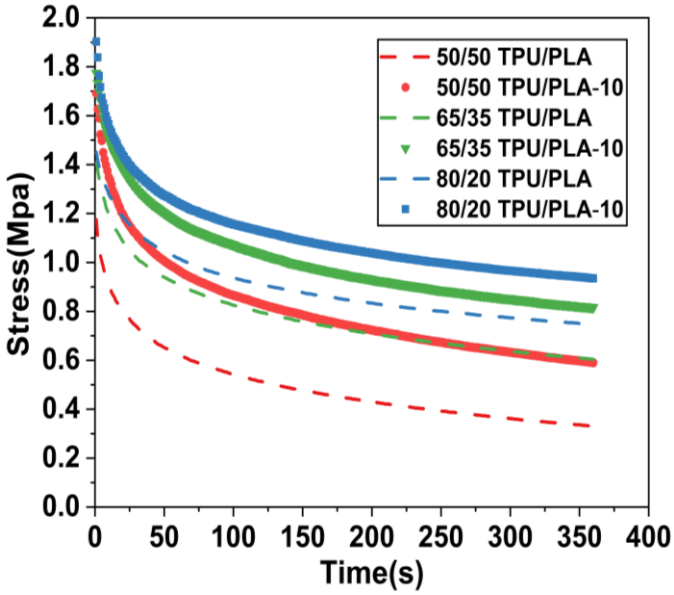

Figure 7.4 Stress Relaxation for polymer composites with 0% and 10% BN filler under tension

Figure 7.5 illustrates the stress relaxation curves of the samples, where the polymer composites containing 10 wt.% h-BN as filler are represented by dense dots, while those without h-BN are denoted by dashed lines for clarity. The graph demonstrates that the incorporation of 10 wt.% h-BN as filler leads to higher stresses for all compositions of TPU/PLA samples. In particular, for the 50/50 TPU/PLA samples exhibit the greatest difference in stress, observed with the addition of BN.

Sample	0min Stress [MPa]	6min Stress [MPa]
50/50 TPU/PLA	1.17	0.33
50/50 TPU/PLA-10	1.69	0.59
65/35 TPU/PLA	1.41	0.60
65/35 TPU/PLA-10	1.77	0.82
80/20 TPU/PLA	1.45	0.75
80/20 TPU/PLA-10	1.90	0.93

Table 7.6 Initial and final stresses for polymer composites with 0% and 10% BN filler in the process of stress relaxation

The current findings align with previous observations, emphasizing that the addition of h-BN as a filler result in higher stored internal stresses. This impact of h-BN is particularly pronounced for samples with lower initial stress, which means the stress at 0 min stretching time. By incorporating h-BN, the internal stress could be adjusted to achieve the desired higher level. For instance, as illustrated in Figure 7.4, the 50/50 TPU/PLA composite loaded with 10 wt.% h-BN achieves a stress level similar to that of 65/35 TPU/PLA sample with no h-BN added.

7.3.2.2 Characterization of Shape Memory Effect

Measurements of the shape memory properties of polymer composites with or without h-

BN are shown below in Figure 7.5. This section compares 50/50 TPU/PLA, 65/35 TPU/PLA, and 80/20 TPU/PLA polymer blends to their respective composites filled with 10 wt.% h-BN. Dashed lines represent samples without h-BN filler, while solid lines indicate composites filled with 10 wt.% h-BN.

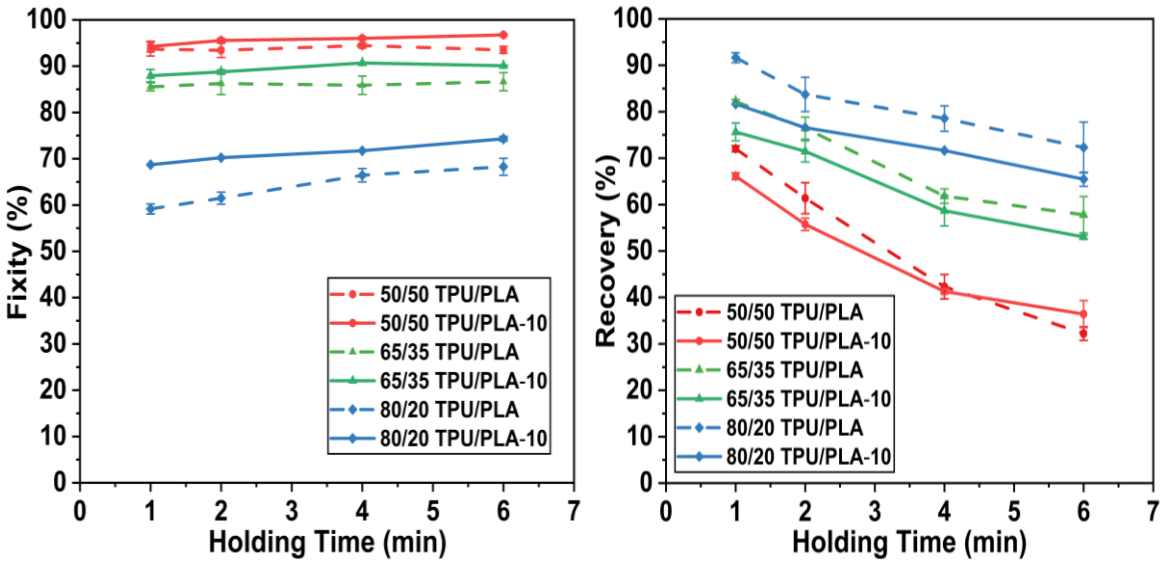

(a) (b)

Figure 7.5 Shape memory effect characterization of polymer composites with 0% and 10% BN filler: (a) fixity (b) recovery

Figure 7.6 depicts the fixity and recovery of these samples. As anticipated, the addition of 10 wt.% h-BN results in a consistent alternation across all composites. When filled with 10 wt.% BN, the polymer composites achieve higher fixity and generally lower recovery. Interestingly, contrary to the stress relaxation characterization, the impact of adding 10 wt.% h-BN appears to

be more pronounced on the shape memory properties of samples with higher TPU content. Notably, the variation between 80/20 TPU/PLA and 80/20 TPU/PLA-10 composites can reach up to 5 to 10% (as indicated in Table 7.7), while differences in samples with other compositions remain around ~3%. This disparity might be attributed to h-BN's influence on the interactions in TPU. h-BN within TPU seems to function more as barriers, hindering the movement of polymer chains rather than actively contributing to building stronger networks.

Holding time [min] / Sample	1	2	4	6
50/50 TPU/PLA	93.7 ± 1.50	93.43 ± 1.54	94.44 ± 0.51	93.53 ± 0.74
50/50 TPU/PLA-10	94.25 ± 1.15	95.55 ± 0.41	96.02 ± 0.31	96.76 ± 0.25
65/35 TPU/PLA	85.54 ± 0.87	86.25 ± 2.39	85.88 ± 1.99	86.65 ± 1.96
65/35 TPU/PLA-10	87.95 ± 1.34	88.76 ± 0.43	90.70 ± 0.08	90.11 ± 0.13
80/20 TPU/PLA	59.44 ± 1.14	61.32 ± 1.55	66.50 ± 1.74	67.99 ± 2.14
80/20 TPU/PLA-10	68.00 ± 1.01	70.84 ± 0.87	74.69 ± 0.52	74.32 ± 0.52

(a)

Table 7.7 shape memory effect characterization values of polymer composites with 0% and 10% BN filler: (a) fixity (b) recovery

Holding time [min] / Sample	1	2	4	6
50/50 TPU/PLA	72.03 ± 0.66	61.38 ± 3.34	42.31 ± 2.63	32.21 ± 1.46
50/50 TPU/PLA-10	66.12 ± 0.72	55.76 ± 1.32	41.30 ± 0.55	36.41 ± 2.92
65/35 TPU/PLA	82.20 ± 0.45	76.45 ± 2.38	61.84 ± 1.54	57.82 ± 3.92
65/35 TPU/PLA-10	75.65 ± 1.92	71.48 ± 2.29	58.69 ± 3.29	53.02 ± 0.44
80/20 TPU/PLA	91.30 ± 1.01	82.49 ± 3.39	77.74 ± 2.70	71.07 ± 5.98
80/20 TPU/PLA-10	81.11 ± 0.79	77.18 ± 0.88	70.83 ± 1.15	65.47 ± 1.51

(b)

Table 7.7 shape memory effect characterization values of polymer composites with 0% and 10% BN filler: (a) fixity (b) recovery [continue]

The correlation between the h-BN filler and the composition of the TPU and PLA components in the polymer blend is the focus of the subsequent investigation. In Figure 7.6, the fixity and recovery of samples with and without 10 wt.% h-BN added are shown, using 1 minute and 6 minutes as representative of the stretching time. Experimental results clearly illustrate that samples with and without 10 wt.% h-BN exhibit similar trends, indicating an increase in fixity and a decrease in recovery. While the addition of h-BN as a filler in the polymer blends might impact the magnitude of the shape memory properties, it can be assumed that it does not significantly alter the underlying mechanism of the polymer composite, given that the trends remain relatively

unchanged with the increase in PLA content.

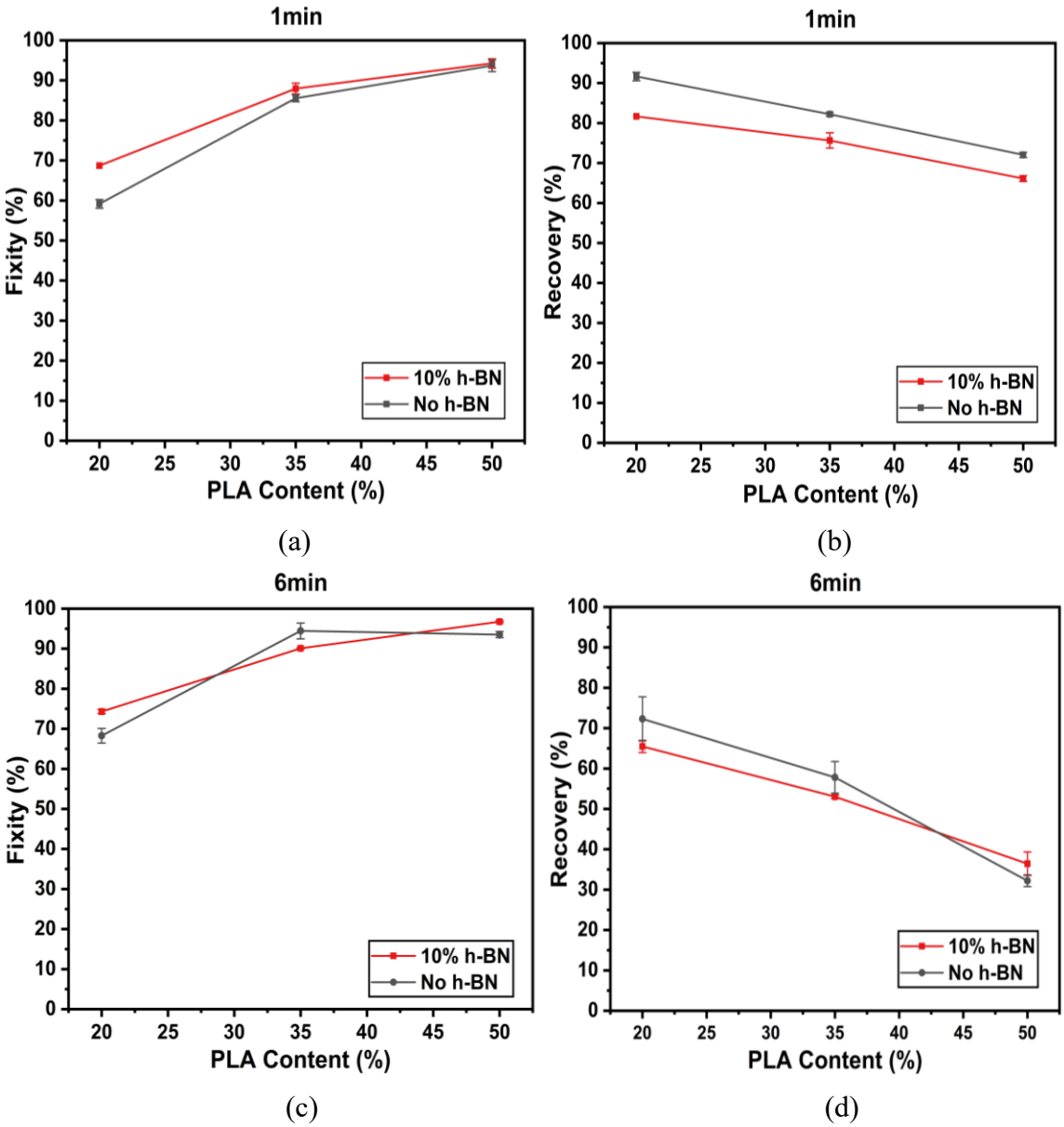

Figure 7.6 Shape memory effect characterization of polymer composites with varying h-BN and PLA content: (a) (b) with 1min stretching time (c) (d) with 6min stretching time

7.4 Conclusion

Two parts of study in this chapter aim to investigate the effects of incorporating h-BN into the TPU/PLA polymer blends on their shape memory effects. In the first part, varying amounts of h-BN ranging from 0 wt.% to 10 wt.% were added as filler to the TPU/PLA polymer blends. Higher h-BN content led to higher internal stress stored after stretching, accompanied by a decrease in melt crystallinity. Among these samples, significant changes in shape memory properties were observed only in TPU50/PLA50/BN10 sample, exhibiting higher fixity and lower recovery. The other samples displayed less noticeable differences.

Building upon these results, Part 2 focused solely on polymer blends loaded with 10 wt.% h-BN across all blend compositions – 50/50 TPU/PLA-10, 65/35 TPU/PLA-10 and 80/20 TPU/PLA-10. The addition of 10 wt.% h-BN consistently induced alternations in the properties of these samples, including higher stored stress, increased fixity, and lower recovery. Notably, samples with higher TPU content showed more pronounced changes in shape memory properties, suggesting that h-BN more effectively modifies the shape memory performance of samples with higher TPU contents.

In summary, this chapter elucidates the effect of h-BN addition to TPU/PLA polymer blends. The results show that h-BN only led to noticeable effects at high loading, particularly at10

wt.%, enhancing the ability to fix temporary shapes while diminishing recovery. This characteristic can be leveraged to develop TPU/PLA composites with improved fixity. Hence, combining these two conditions could be envisaged to achieve the desired shape memory properties in TPU/PLA polymer composites.

Chapter 8. Summary

8.1 Summary and Conclusion

This study delves into investigating the working mechanism and the associated shape memory properties of thermoplastic polyurethane (TPU)/polylactic acid (PLA)-based shape memory polymer composites. In the first part of the research, a fundamental study was conducted on TPU/PLA polymer blends with different compositions. By adjusting the PLA content within the polymer blends, the study elucidates the distinct roles of each component in achieving the shape memory effect and identifies the pivotal microstructural factors influencing the shape memory properties, namely the TPU phase as well as the crystalline and amorphous regions of PLA. The TPU phase as well as the crystalline region of PLA work together as the permanent phase in the shape memory system of the polymer blend facilitating shape recovery. While the amorphous region of PLA serves as the reversible phase and is responsible for fixing the temporary shape. The findings underscore that higher TPU content leads to higher internal storage stress and consequently greater recovery, while PLA significantly contributes to fixity.

The second part of this research examined the effect of stretching duration at the transition

temperature within the shape memory test cycle on the shape memory properties of the TPU/PLA blends. As a crucial step involves in the shape memory test cycle, the stretching time holds considerable potential in governing the final exhibited shape memory properties. The findings illustrate a noteworthy trend: an increase in the holding time leads to a significant reduction in recovery while marginally enhancing fixity. In addition, this investigation offers a clearer and more comprehensive understanding of the specific contribution of influential factors in the mechanism, especially the degree of crystallinity and the internal stress.

The third part of this study focuses on exploring the influence of different cooling methods during sample preparation on the shape memory effect. This specifically refers to the cooling process after the compression molding step, which is presumed to have a direct impact on the crystalline structure of the polymer blend. Slower cooling rate led to an increase in the initial degree of crystallinity within the polymer blend, thereby bolstering recovery and reducing the dependence of shape memory properties on variations in stretching time. However, the fixity of polymer blends subjected to slower cooling rate was simultaneously affected to decrease. Moreover, a distinction is drawn between crystals induced by stretching and those formed during the cooling process, elucidating their individual contributions to the shape memory properties.

The final part of this study involves introducing hexagonal boron nitride (h-BN) as a filler in TPU/PLA polymer blends to further improve their properties. This represents a new attempt as addition of h-BN has yet been explored in the research on shape memory polymer. The results indicate that significant effects of h-BN addition are primarily observable at higher h-BN contents, notably at 10 wt.% h-BN. Fixity demonstrates improvement with the addition of h-BN, albeit accompanied by a decline in recovery. Furthermore, the study elucidates that the introduction of h-BN is likely to disrupt the physical network of TPU.

In summary, the main contributions of this study can be outlined below:

1. In shape memory TPU/PLA polymer blends, both the TPU as well as the crystalline phase of PLA serve as the permanent phase for energy storage and facilitating recovery. Conversely, the amorphous domain of PLA serves as the reversible phase responsible for affecting phase change and plays a crucial role in fixity. Consequently, an increase in TPU content corresponds to enhanced recovery but reduced fixity.
2. The duration of holding time in stretching the samples during the shape memory test cycle significantly impacts the degree of crystallinity and stored stresses within polymer blends. In the context of a 50/50 TPU/PLA polymer blend, extending the stretching time from 0

minute to 6 minutes promoted the degree of crystallinity in PLA from 7.8% to 42.7%. Conversely, the internal stress decreased from 1.17 MPa to 0.33 MPa. Consequently, this reduction in internal stress diminished the ability of the polymer blends to recover and marginally enhance their fixity. In particular, polymer blends with higher PLA content were more susceptible to the influence of stretching time, resulting in a more pronounced decrease in the recovery.

3. In exploring the effect of stretching duration, detailed analyses were conducted to examine the degrees of crystallinity in the polymer blends. The crystals formed during the stretching phase in the shape memory tests exhibited contrasting roles compared to the initial crystals inherent in the polymer blends upon their fabrication. In this Scenario, the crystals generated by stretching, along with the amorphous domain of the PLA, collaborated to contribute to the sample's fixity, while the inherent crystals and the TPU component play a role in the shape recovery.
4. Employing a slower cooling rate for sample preparation resulted in a significant increase in the degree of crystallinity in the PLA phase. Unlike the crystals generated in the stretching process, these promoted crystallinities were recognized as the initial crystals

existing prior to shape memory programming process. Consequently, an increase in the crystallinity of such crystals led to higher stored stress and facilitated recovery. However, it was found that the fixity was suppressed. More importantly, the shape memory properties of sample subjected to slow cooling appeared to be more consistent and less sensitive to changes in composition and stretching time.

5. The addition of h-BN particles introduced an additional parameter to be considered within the current shape memory system. Unlike the crystals, h-BN could affect the microstructure of not only TPU, but also PLA. The presence of h-BN would interfere with the physical networking in TPU, as well as the crystallization of PLA due to heterogeneous nucleation. Moreover, incorporating h-BN in the material system could lead to greater stress storage within the polymer composite.
6. The effect of h-BN on the shape memory properties became more visible at comparatively higher loadings (e.g., 10 wt.%). The addition of h-BN improved fixity but concurrently reduced recovery. Notably, polymer composites with hither TPU content exhibited slightly more pronounced effects under these circumstances.

8.2 Scope for Future Work

This study systematically elucidates the working mechanism governing the shape memory effect within TPU/PLA blends. It effectively establishes the correlations between specific factors and the resultant shape memory properties. The outcomes of this investigation suggest several promising directions for further exploration and research:

1. At present, several research endeavours concentrate on TPU/PLA-based shape memory polymer composites, showing promise for diverse applications through tailored modifications. While shape memory characterization remains essential in these studies, there is a prevailing inadequacy in addressing the intricacies of the shape memory testing process. In general, attention has been cursorily allocated to the study of programming temperature. In contrast, this study has revealed that stretching time represents another crucial parameter in the shape memory programming cycle governing the shape memory properties. It is believed that there are still many other parameters in the shape memory test cycle holding significant potent for further investigation. Some examples include the tensile rate and the post-deformation cooling rate. Comprehending and managing these variables stand to standardize the programming process, leading to more consistent

performance and reliable.

2. The present study has highlighted contrasting effects of several conditions on shape memory properties, such as slower cooling rates and longer stretching times. Therefore, there is an anticipation to devise an analytical model capable of accurately predicting the shape memory properties by manipulating these conditions in experimental setups. Such a model would enable the tailoring of shape memory properties to accommodate the needs of specific applications, enabling precise customization.
3. Given the relative scarcity of h-BN in studies related to shape memory polymer composites, there remains ample room for further exploration concerning its addition. For instance, investigating the effect of particle sizes of h-BN could potentially identify another path to tune the shape memory properties. Furthermore, exploring the effect of h-BN or other thermal conductivity fillers on the speed of shape recovery can also provide new insights for specific applications.

REFERENCES

[1] W. M. Huang, Z. Ding, C. C. Wang, J. Wei, Y. Zhao, H. Purnawali, *Mater. Today* **2010**, *13*, 54.

[2] M. Behl, A. Lendlein, *Mater. Today* **2007**, *10*, 20.

[3] J. Mohd Jani, M. Leary, A. Subic, M. A. Gibson, *Mater. Des. 1980-2015* **2014**, *56*, 1078.

[4] D. Mantovani, *JOM* **2000**, *52*, 36.

[5] L. G. Machado, M. A. Savi, *Braz. J. Med. Biol. Res.* **2003**, *36*, 683.

[6] G. Song, N. Ma, H.-N. Li, *Eng. Struct.* **2006**, *28*, 1266.

[7] Barik S. K., Rao D. P. S., *Int. J. Eng. Res. Technol.* **2019**, *7*.

[8] M. R. Ahmad, M. H. M. Yahya, M. R. Hassan, J. Salleh, W. Y. W. Ahmad, N. Hassim, in *2012 IEEE Business, Engineering & Industrial Applications Colloquium (BEIAC)*, IEEE: Kuala Lumpur, Malaysia, **2012**, pp 216.

[9] D. J. Hartl, D. C. Lagoudas, *Proc. Inst. Mech. Eng. Part G J. Aerosp. Eng.* **2007**, *221*, 535.

[10] D. Stoeckel, *Mater. Des.* **1990**, *11*, 302.

[11] M. O. Gök, M. Z. Bilir, B. H. Gürcüm, *Procedia - Soc. Behav. Sci.* **2015**, *195*, 2160.

[12] A. Gupta, A. Maharjan, B. S. Kim, *Appl. Sci.* **2019**, *9*, 4694.

[13] A. Lendlein, S. Kelch, *Angew. Chem. Int. Ed.* **2002**, *41*, 2034.

[14] T. Tsonev, S. Nenkova, M. Herzog, **2014**.

[15] P. T. Mather, X. Luo, I. A. Rousseau, *Annu. Rev. Mater. Res.* **2009**, *39*, 445.

[16] W. Sokolowski, A. Metcalfe, S. Hayashi, L. Yahia, J. Raymond, *Biomed. Mater.* **2007**, *2*, S23.

[17] C. Liu, H. Qin, P. T. Mather, *J. Mater. Chem.* **2007**, *17*, 1543.

[18] M. D. Hager, S. Bode, C. Weber, U. S. Schubert, *Prog. Polym. Sci.* **2015**, *49–50*, 3.

[19] H. Liu, Q. Li, S. Zhang, R. Yin, X. Liu, Y. He, K. Dai, C. Shan, J. Guo, C. Liu, C. Shen, X. Wang, N. Wang, Z. Wang, R. Wei, Z. Guo, *J. Mater. Chem. C* **2018**, *6*, 12121.

[20] L. Li, P. Shi, L. Hua, J. An, Y. Gong, R. Chen, C. Yu, W. Hua, F. Xiu, J. Zhou, G. Gao, Z. Jin, G. Sun, W. Huang, *Nanoscale* **2018**, *10*, 118.

[21] X. Li, M. J. Serpe, *Adv. Funct. Mater.* **2016**, *26*, 3282.

[22] L. Sun, T. X. Wang, H. M. Chen, A. V. Salvekar, B. S. Naveen, Q. Xu, Y. Weng, X. Guo, Y. Chen, W. M. Huang, *Polymers* **2019**, *11*, 1049.

[23] F. Quadrini, D. Bellisario, L. Iorio, L. Santo, *Mater. Res. Express* **2019**, *6*, 115711.

[24] L. Santo, F. Quadrini, A. Accettura, W. Villadei, *Procedia Eng.* **2014**, *88*, 42.

[25] Y. Xia, Y. He, F. Zhang, Y. Liu, J. Leng, *Adv. Mater.* **2021**, *33*, 2000713.

[26] J. Delaey, P. Dubruel, S. Van Vlierberghe, *Adv. Funct. Mater.* **2020**, *30*, 1909047.

[27] B. Kumar, N. Noor, S. Thakur, N. Pan, H. Narayana, S. Yan, F. Wang, P. Shah, *ACS Omega* **2019**, *4*, 15348.

[28] J. Hu, *Shape Memory Polymers and Textiles*, Elsevier, **2007**.

[29] Shape Memory Polymer Market Share and Statistics – 2032. *Glob. Mark. Insights Inc*. https://www.gminsights.com/industry-analysis/shape-memory-polymer-market (accessed

December 3, 2023).

[30] Y. Li, Z. Liu, *Polymer* **2018**, *143*, 298.

[31] K. Yu, H. J. Qi, *Soft Matter* **2014**, *10*, 9423.

[32] J. Hu, S. Chen, *J. Mater. Chem.* **2010**, *20*, 3346.

[33] T. Dayyoub, A. V. Maksimkin, O. V. Filippova, V. V. Tcherdyntsev, D. V. Telyshev, *Polymers* **2022**, *14*, 3511.

[34] X. Xiao, J. Hu, X. Gui, K. Qian, *Polymers* **2017**, *9*, 87.

[35] K. Strzelec, N. Sienkiewicz, T. Szmechtyk, in *Shape Memory Polymers, Blends and Composites: Advances and Applications* (Eds.: J. Parameswaranpillai, S. Siengchin, J. J. George, S. Jose), Advanced Structured Materials, Springer: Singapore, **2020**, pp 21.

[36] J. Hu, Y. Zhu, H. Huang, J. Lu, *Prog. Polym. Sci.* **2012**, *37*, 1720.

[37] M. C. Choi, J.-Y. Jung, Y.-W. Chang, *Polym. Bull.* **2014**, *71*, 625.

[38] F. Li, Y. Chen, W. Zhu, X. Zhang, M. Xu, *Polymer* **1998**, *39*, 6929.

[39] J. W. Cho, J. W. Kim, Y. C. Jung, N. S. Goo, *Macromol. Rapid Commun.* **2005**, *26*, 412.

[40] D. Habault, H. Zhang, Y. Zhao, *Chem. Soc. Rev.* **2013**, *42*, 7244.

[41] M. Herath, J. Epaarachchi, M. Islam, L. Fang, J. Leng, *Eur. Polym. J.* **2020**, *136*, 109912.

[42] A. Lendlein, H. Jiang, O. Jünger, R. Langer, *Nature* **2005**, *434*, 879.

[43] S. J. M. van Vilsteren, H. Yarmand, S. Ghodrat, *Magnetochemistry* **2021**, *7*, 123.

[44] W. Zhao, Z. Huang, L. Liu, W. Wang, J. Leng, Y. Liu, *Compos. Sci. Technol.* **2021**, *203*, 108563.

[45] D. L. Safranski, K. Gall, *Polymer* **2008**, *49*, 4446.

[46] W. Hu, Z. Wang, Y. Xiao, S. Zhang, J. Wang, *Biomater. Sci.* **2019**, *7*, 843.

[47] R. A. Weiss, E. Izzo, S. Mandelbaum, *Macromolecules* **2008**, *41*, 2978.

[48] Y. Chen, C. Chen, H. U. Rehman, X. Zheng, H. Li, H. Liu, M. S. Hedenqvist, *Molecules* **2020**, *25*, 4246.

[49] K. Yu, Q. Ge, H. J. Qi, *Nat. Commun.* **2014**, *5*, 3066.

[50] M. Zare, M. P. Prabhakaran, N. Parvin, S. Ramakrishna, *Chem. Eng. J.* **2019**, *374*, 706.

[51] S. Chen, J. Hu, H. Zhuo, Y. Zhu, *Mater. Lett.* **2008**, *62*, 4088.

[52] C. Samuel, S. Barrau, J.-M. Lefebvre, J.-M. Raquez, P. Dubois, *Macromolecules* **2014**, *47*, 6791.

[53] I. A. Rousseau, *Polym. Eng. Sci.* **2008**, *48*, 2075.

[54] S. P. Dubey, V. K. Thakur, S. Krishnaswamy, H. A. Abhyankar, V. Marchante, J. L. Brighton, *Vacuum* **2017**, *146*, 655.

[55] M. Jamshidian, E. A. Tehrany, M. Imran, M. Jacquot, S. Desobry, *Compr. Rev. Food Sci. Food Saf.* **2010**, *9*, 552.

[56] A. J. R. Lasprilla, G. A. R. Martinez, B. H. Lunelli, A. L. Jardini, R. M. Filho, *Biotechnol. Adv.* **2012**, *30*, 321.

[57] M. Mehrpouya, H. Vahabi, S. Janbaz, A. Darafsheh, T. R. Mazur, S. Ramakrishna, *Polymer* **2021**, *230*, 124080.

[58] F. S. Senatov, K. V. Niaza, M. Yu. Zadorozhnyy, A. V. Maksimkin, S. D. Kaloshkin, Y. Z.

Estrin, *J. Mech. Behav. Biomed. Mater.* **2016**, *57*, 139.

[59] E. Waris, Y. T. Konttinen, N. Ashammakhi, R. Suuronen, S. Santavirta, *Expert Rev. Med. Devices* **2004**, *1*, 229.

[60] D. Nie, X. Yin, Z. Cai, J. Wang, *Polymers* **2022**, *14*, 1569.

[61] J. Li, X. Zhao, L. Ye, P. Coates, F. Caton-Rose, *J. Biomed. Mater. Res. A* **2019**, *107*, 872.

[62] H.-Y. Mi, M. R. Salick, X. Jing, B. R. Jacques, W. C. Crone, X.-F. Peng, L.-S. Turng, *Mater. Sci. Eng. C Mater. Biol. Appl.* **2013**, *33*, 4767.

[63] S. Qian, K. Sheng, *Compos. Sci. Technol.* **2017**, *148*, 59.

[64] D. R. Paul, *Polymer Blends Volume 1*, Elsevier, **2012**.

[65] D. K. Chattopadhyay, K. V. S. N. Raju, *Prog. Polym. Sci.* **2007**, *32*, 352.

[66] M. Nofar, M. Mohammadi, P. J. Carreau, *J. Appl. Polym. Sci.* **2020**, *137*, 49387.

[67] L. Wan, C. Deng, H. Chen, Z.-Y. Zhao, S.-C. Huang, W.-C. Wei, A.-H. Yang, H.-B. Zhao, Y.-Z. Wang, *Chem. Eng. J.* **2021**, *417*, 129314.

[68] Q. Yuan, T. Zhou, L. Li, J. Zhang, X. Liu, X. Ke, A. Zhang, *RSC Adv.* **2015**, *5*, 31153.

[69] S. Boyacioglu, M. Kodal, G. Ozkoc, *Eur. Polym. J.* **2020**, *122*, 109372.

[70] W. Wang, X. Liao, F. Guo, G. Wang, Z. Yan, F. Liu, G. Li, *Ind. Eng. Chem. Res.* **2020**, *59*, 7611.

[71] S. K. Dogan, S. Boyacioglu, M. Kodal, O. Gokce, G. Ozkoc, *J. Mech. Behav. Biomed. Mater.* **2017**, *71*, 349.

[72] J. J. Song, I. Srivastava, J. Kowalski, H. E. Naguib, in (Eds.: N. C. Goulbourne, H. E.

Naguib), San Diego, California, USA, **2014**, p 90580B.

[73] X. Jing, H.-Y. Mi, M. R. Salick, T. Cordie, W. C. Crone, X.-F. Peng, L.-S. Turng, *J. Cell. Plast.* **2014**, *50*, 361.

[74] X. Jing, H.-Y. Mi, X.-F. Peng, L.-S. Turng, *Polym. Eng. Sci.* **2015**, *55*, 70.

[75] Y. Guo, L. Yan, Z. Zeng, L. Chen, M. Ma, R. Luo, J. Bian, H. Lin, D. Chen, *Polym. Eng. Sci.* **2020**, *60*, 1118.

[76] T. Liu, R. Huang, X. Qi, P. Dong, Q. Fu, *Polymer* **2017**, *114*, 28.

[77] F. Azadi, S. H. Jafari, H. A. Khonakdar, M. Arjmand, U. Wagenknecht, V. Altstädt, *Macromol. Mater. Eng.* **2021**, *306*, 2000576.

[78] X. Qi, H. Xiu, Y. Wei, Y. Zhou, Y. Guo, R. Huang, H. Bai, Q. Fu, *Compos. Sci. Technol.* **2017**, *139*, 8.

[79] G. Wu, B. Li, J. Jiang, *Polymer* **2010**, *51*, 2077.

[80] H. Xiu, C. Huang, H. Bai, J. Jiang, F. Chen, H. Deng, K. Wang, Q. Zhang, Q. Fu, *Polymer* **2014**, *55*, 1593.

[81] J. Wang, F. Ma, W. Liang, M. Sun, *Mater. Today Phys.* **2017**, *2*, 6.

[82] J. Eichler, C. Lesniak, *J. Eur. Ceram. Soc.* **2008**, *28*, 1105.

[83] A. E. Naclerio, P. R. Kidambi, *Adv. Mater.* **2023**, *35*, 2207374.

[84] M. Dadvand, O. Savadogo, *Coatings* **2022**, *12*, 1011.

[85] Y. Wang, H. Jin, J. Shen, B. Wang, X. Feng, Z. Mao, Y. Zhang, X. Sui, *J. Mater. Sci. Technol.* **2022**, *101*, 146.

[86] S. D. Ostrovskiy, I. A. Krotenko, A. A. Stepashkin, M. Yu. Zadorozhnyy, D. A. Kiselev, T. S. Ilina, E. A. Kolesnikov, F. S. Senatov, *Polym. Compos. n/a*.

[87] R. Ayoob, F. Alhabill, T. Andritsch, A. Vaughan, *J. Mater. Sci.* **2018**, *53*, 3427.

[88] J. Li, J. Leng, Y. Jiang, J. Zhang, *Compos. Part Appl. Sci. Manuf.* **2021**, *150*, 106586.

[89] X. Zhao, L. Ye, P. Coates, F. Caton-Rose, M. Martyn, *Polym. Adv. Technol.* **2013**, *24*, 853.

[90] R. M. R. Wellen, M. S. Rabello, I. C. Araujo Júnior, G. J. M. Fechine, E. L. Canedo, *Polímeros* **2015**, *25*, 296.

[91] Y. Hu, Y. Liao, Y. Zheng, K. Ikeda, R. Okabe, R. Wu, R. Ozaki, J. Xu, Q. Xu, *Polymers* **2022**, *14*, 3646.

[92] Y. Hu, Y. S. Hu, V. Topolkaraev, A. Hiltner, E. Baer, *Polymer* **2003**, *44*, 5681.

[93] R. B. D. Cunha, F. R. Pê, P. Agrawal, G. D. Figueiredo Brito, T. J. A. De Mélo, *Smart Mater. Struct.* **2023**, *32*, 085016.

[94] S.-M. Lai, Y.-C. Lan, *J. Polym. Res.* **2013**, *20*, 140.

[95] J. J. Song, H. H. Chang, H. E. Naguib, *Eur. Polym. J.* **2015**, *67*, 186.

[96] K. Akhtar, S. A. Khan, S. B. Khan, A. M. Asiri, in *Handbook of Materials Characterization* (Ed.: S. K. Sharma), Springer International Publishing: Cham, **2018**, pp 113.

[97] A. Mohammed, A. Abdullah.

[98] W. Zhou, R. P. Apkarian, Z. L. Wang, D. Joy.

[99] C. Schick, *Anal. Bioanal. Chem.* **2009**, *395*, 1589.

[100] F. Carrasco, O. Santana Pérez, M. L. Maspoch, *Polymers* **2021**, *13*, 3996.

[101] B. Gupta, N. Revagade, J. Hilborn, *Prog. Polym. Sci.* **2007**, *32*, 455.

[102] Q. Wang, A. Shi, F. Shah, in *Evaluation Technologies for Food Quality* (Eds.: J. Zhong, X. Wang), Woodhead Publishing Series in Food Science, Technology and Nutrition, Woodhead Publishing, **2019**, pp 465.

[103] B. Huneau, *Rubber Chem. Technol.* **2011**, *84*, 425.

[104] M. Salmerón Sánchez, V. B. F. Mathot, G. Vanden Poel, J. L. Gómez Ribelles, *Macromolecules* **2007**, *40*, 7989.

[105] N. Uthaipan, M. Jarnthong, Z. Peng, B. Junhasavasdikul, C. Nakason, A. Thitithammawong, *Polym. Test.* **2015**, *44*, 101.

[106] S. Oshima, R. Higuchi, M. Kato, S. Minakuchi, T. Yokozeki, T. Aoki, *Compos. Part Appl. Sci. Manuf.* **2023**, *164*, 107250.

[107] J. Wootthikanokkhan, T. Cheachun, N. Sombatsompop, S. Thumsorn, N. Kaabbuathong, N. Wongta, J. Wong-On, S. I. Na Ayutthaya, A. Kositchaiyong, *J. Appl. Polym. Sci.* **2013**, *129*, 215.

[108] K. Sahakaro, in *Progress in Rubber Nanocomposites* (Eds.: S. Thomas, H. J. Maria), Woodhead Publishing Series in Composites Science and Engineering, Woodhead Publishing, **2017**, pp 81.